Title

Combinatorial Complexity in a Transcriptionally Centered Signaling Hub in Arabidopsis

Journal

Molecular Plant, 7(11)

ISSN

1674-2052

Authors

Pfeiffer, Anne
Shi, Hui
Tepperman, James M
et al.

Publication Date

2014-11-01

DOI

10.1093/mp/ssu087

Peer reviewed

Combinatorial Complexity in a Transcriptionally Centered Signaling Hub in *Arabidopsis*

Anne Pfeiffer[a,b], **Hui Shi**[a,b], **James M. Tepperman**[a,b], **Yu Zhang**[a,b], and **Peter H. Quail**[a,b,1]

a Department of Plant and Microbial Biology, University of California, Berkeley, CA 94720, USA
b United States Department of Agriculture, Plant Gene Expression Center, Albany, CA 94710, USA

ABSTRACT **A subfamily of four Phytochrome (phy)-Interacting bHLH transcription Factors (PIFs) collectively promote skotomorphogenic development in dark-grown seedlings. This activity is reversed upon exposure to light, by photoactivated phy molecules that induce degradation of the PIFs, thereby triggering the transcriptional changes that drive a transition to photomorphogenesis. The PIFs function both redundantly and partially differentially at the morphogenic level in this process. To identify the direct targets of PIF transcriptional regulation genome-wide, we analyzed the DNA-binding sites for all four PIFs by ChIP-seq analysis, and defined the genes transcriptionally regulated by each PIF, using RNA-seq analysis of *pif* mutants. Despite the absence of detectable differences in DNA-binding-motif recognition between the PIFs, the data show a spectrum of regulatory patterns, ranging from single PIF dominance to equal contributions by all four. Similarly, a broad array of promoter architectures was found, ranging from single PIF-binding sites, containing single sequence motifs, through multiple PIF-binding sites, each containing one or more motifs, with each site occupied preferentially by one to multiple PIFs. Quantitative analysis of the promoter occupancy and expression level induced by each PIF revealed an intriguing pattern. Although there is no robust correlation broadly across the target-gene population, examination of individual genes that are shared targets of multiple PIFs shows a gradation in correlation from strongly positive, through uncorrelated, to negative. This finding suggests a dual-layered mechanism of transcriptional regulation, comprising both a continuum of binding-site occupancy by each PIF and a superimposed layer of local regulation that acts differentially on each PIF, to modulate its intrinsic transcriptional activation capacity at each site, in a quantitative pattern that varies between the individual PIFs from gene to gene. These findings provide a framework for probing the mechanisms by which transcription factors with overlapping direct-target genes integrate and selectively transduce signals to their target networks.**

Key words: phytochromes; light-signaling; PIFs; bHLH transcription factors; promoter occupancy; *Arabidopsis*; transcriptional regulation; ChIP-seq; RNA-seq.

Pfeiffer A.,Shi H.,Tepperman J.M.,Zhang Y.,Quail P.H.,(2014).Combinatorial complexity in a transcriptionally centered signaling hub in *Arabidopsis*.Mol. Plant. 7, 1598–1618.

INTRODUCTION

Terrestrial flowering plants have evolved a developmental strategy termed skotomorphogenesis that enables seedlings germinating from buried seed to grow rapidly upward on stored energy reserves, in the subterranean darkness, to the soil surface (Schäfer and Nagy, 2006; Franklin and Quail, 2010). In dicots, such as *Arabidopsis*, this strategy is displayed at the visible phenotypic level as long hypocotyls, closed apical hooks, and small, unexpanded, appressed cotyledons. At the cellular level, this phenotype is displayed as concomitant, rapid hypocotyl-cell elongation and suppressed cotyledon cell expansion. Emergence into the light initiates the well-known transition to photomorphogenic development (termed deetiolation), displayed as inhibition of hypocotyl elongation, unfolding of the apical hook, separation and expansion of the cotyledons, and development of photosynthetically active chloroplasts (Quail, 2002; Wang and Deng, 2003; Franklin and Quail, 2010).

[1] To whom correspondence should be addressed. E-mail quail@berkeley.edu, fax 510-559–5678, tel. 510-559–5900

doi:10.1093/mp/ssu087 Advance Access publication 13 August 2014
Received 6 May 2014; accepted 29 July 2014

Assembled genetic evidence shows that a quartet of bHLH transcription factors, called PIF1, PIF3, PIF4, and PIF5 (for *P*hytochrome (phy)-*I*nteracting *F*actors (PIFs)), have a central functional role in promoting the skotomorphogenic pathway (Toledo-Ortiz et al., 2003; Duek and Fankhauser, 2005; Castillon et al., 2007; Quail, 2007; Leivar and Quail, 2011). A quadruple *pif* mutant (*pifq*), lacking these four PIFs (collectively called the 'PIF quartet'), displays development in total darkness that strongly phenocopies that of normal light-grown wild-type (WT) seedlings, thereby establishing that the quartet functions constitutively to sustain skotomorphogenesis (Leivar et al., 2008; Shin et al., 2009). Moreover, initial exposure to light triggers a rapid decline in PIF-quartet protein levels (half-times of 5–20 min) (Bauer et al., 2004; Park et al., 2004; Shen et al., 2005; Al-Sady et al., 2006; Oh et al., 2006; Nozue et al., 2007; Shen et al., 2007; Lorrain et al., 2008; Shen et al., 2008), reversing their promotive activity, and consequently initiating the switch from skotomorphogenic to photomorphogenic development (Leivar et al., 2008; Shin et al., 2009). The light signal that induces this response is perceived by members of the phytochrome (phy) family of sensory photoreceptors (predominantly phyA and phyB) (Rockwell et al., 2006; Bae and Choi, 2008). Photoactivation of the phy molecule induces its translocation from the cytoplasm into the nucleus (Nagatani, 2004; Pfeiffer et al., 2012) where it interacts directly with the constitutively nuclear PIF transcription factors (Bauer et al., 2004; Bae and Choi, 2008). This interaction induces rapid transphosphorylation of the PIF-quartet proteins, followed by ubiquitination and proteasome-mediated degradation of these factors (Park et al., 2004; Al-Sady et al., 2006, 2008; Ni et al., 2013). The changes in gene expression induced by this reduction of PIF transcriptional activity then drive the morphological changes associated with deetiolation (Jiao et al., 2007; Quail, 2007).

The available data indicate that the PIFs act pleiotropically in this process. Transcriptome analysis has shown that ~80% of the alterations in gene expression induced in dark-grown *pifq*-mutant seedlings by the absence of the PIF quartet are normally induced by activation of phy signaling upon exposure of WT seedlings to light (Leivar et al., 2008; Shin et al., 2009). Moreover, kinetic analysis of the expression changes induced by initial exposure of dark-grown seedlings to light has shown that rapidly responsive, PIF-quartet-regulated genes are enriched for loci that encode a diversity of transcription factors (Leivar et al., 2008). This suggests a broadly acting, PIF-controlled transcriptional cascade that concomitantly regulates multiple pathways involved in the deetiolation process (Monte et al., 2004; Bae and Choi, 2008; Moon et al., 2008; Lorrain et al., 2009; Shin et al., 2009; Sentandreu et al., 2011). The question of whether and to what extent closely related members of transcription-factor families (such as PIF1, 3, 4, and 5), with a significant degree of apparent functional redundancy at the morphogenic level, contribute to the transcriptional activation of potentially shared target genes, via shared binding to consensus DNA-sequence motifs genome-wide, does not appear to have been widely studied (Boyd et al., 1998; Weinmann et al., 2001; Hollenhorst et al., 2007; Xu et al., 2007; Boros et al., 2009; Farnham, 2009; Hornitschek et al., 2012; Tao et al., 2012).

Recent integrated ChIP-seq and RNA-seq analysis has identified those PIF-quartet-regulated, rapidly light-responsive genes that directly bind PIF3 at sequence-specific target sites (called G-boxes and PBE-boxes) in their promoters, in dark-grown seedlings, and are therefore apparent direct targets of PIF3 transcriptional regulation (Zhang et al., 2013). Similarly, ChIP-seq analysis of PIF5-binding sites genome-wide has identified apparent direct targets of that PIF in light-grown seedlings under shade-avoidance conditions (Hornitschek et al., 2012). How transcription-factor binding to promoters quantitatively determines the expression level of individual target genes is currently an area of considerable interest (Farnham, 2009). It is well recognized that both binding and regulation of the intrinsic activity of bound transcription factors can influence their capacity to regulate transcription of target genes (Zhou and O'Shea, 2011). There is strong evidence from numerous genome-wide binding studies that transcription factors each bind to a majority of genes over a quantitative continuum of DNA occupancy levels, spanning functional, quasifunctional, and nonfunctional DNA-binding events (MacArthur et al., 2009; Biggin, 2011; Cheng et al., 2012; Fisher et al., 2012), and it has been concluded that, in general, differences in regulatory specificities between factors reflect quantitative differences in DNA occupancy levels (Biggin, 2011). Apart from the role of DNA-sequence recognition in binding specificity and affinity, both DNA methylation and nucleosome occlusion of binding sites are well-documented epigenetic inhibitors of transcription-factor binding (Xie et al., 2013). In addition, however, binding of a transcription factor per se is frequently not sufficient for transcriptional regulation, indicating the existence of pervasive post-binding modulation of activity (Farnham, 2009; Zhou and O'Shea, 2011). There is evidence for multiple mechanisms of such modulation, resulting in activation or repression of promoter-bound transcription factors, including posttranslational covalent modification, such as phosphorylation (e.g. yeast Adr1), modulated transcriptional activation domain masking by interacting proteins (e.g. Gal80 occlusion of the Gal4 activation domain blocks recruitment of co-activators), and chaperone-induced allosteric changes (e.g. steroid hormone receptors and Hap1 in yeast) among others (Hahn and Young, 2011). Notably, recent evidence for the yeast Pho4 bHLH factor shows that the activity of this single factor is determined at multiple levels, by a combination of chromatin restriction, competitive binding from the factor Cbf1 that recognizes the same motif as Pho4, and cooperative activation by a co-bound homeodomain transcription

factor, Pho2 (Zhou and O'Shea, 2011). In our recent study (Zhang et al., 2013), initial RT–qPCR analysis of the expression of a selected subset of 14 PIF3-target genes in dark-grown seedlings of all four triple *pif*-mutant combinations revealed a spectrum of differential quantitative contributions of the individual PIF-quartet members, to the collective transcriptional activity of these four PIFs, across these different genes. The extent of the contribution was found to vary both from PIF to PIF, for individual genes, and from gene to gene, for individual PIFs. This finding suggests the possibility of comparable differential activity among the quartet members genome-wide.

We have addressed this possibility here by expanding our investigation to a genome-wide analysis of all four PIF-quartet members, using combined ChIP-seq and RNA-seq data, in order to identify direct targets of transcriptional regulation by each of the individual PIF quartet members, to determine whether these target genes are collectively or individually regulated by the four PIFs, and to quantify the relative contributions of the individual PIFs to the expression of co-regulated genes. Together with the findings of others (Hornitschek et al., 2012; Oh et al., 2012), we provide evidence that the PIF-quartet members share directly in transcriptional activation of numerous target genes, via varying degrees of redundant promoter occupancy, in a manner that varies quantitatively from gene to gene. In addition, we uncover a further layer of regulation that appears to operate independently of the level of promoter occupancy for any given PIF.

RESULTS

Identification of PIF1- and PIF4-Binding Sites by ChIP-Seq Analysis

ChIP-seq-based genome-wide identification of PIF3 (Zhang et al., 2013), PIF4 (Oh et al., 2012), and PIF5 (Hornitschek et al., 2012) DNA-binding sites have been reported. Here we used the same strategy to identify PIF1 and PIF4 binding sites in dark-grown WT seedlings, directly in parallel with RNA-seq-based transcriptome analysis of WT and multiple *pif*-mutant combinations grown together under the same conditions. Dark-grown seedlings expressing MYC-epitope-tagged-PIF1 in a WT background (P1M/PIL5-OX; Oh et al., 2006), MYC-epitope-tagged-PIF4 in a *pif4* null-mutant background (P4M), and untransformed WT control seedlings, were harvested at 2 d, for PIF4-ChIP-seq, and at 3 d for PIF1-ChIP-seq analysis (because of slower germination and development of the P1M seedlings). MYC-antibody immunoprecipitates from three independent biological replicates of each genotype were subjected to high-throughput sequencing, and binding peaks were defined by comparing P1M and P4M samples with the corresponding WT control using MACS software (Zhang et al., 2008). For each reproducible PIF1- and PIF4-specific binding peak, we assigned a common 1-bp summit at the mean position of the replicate-specific summits (Supplemental Table 1). By this analysis, we identified 3027 reproducible binding summits for PIF1 and 2710 for PIF4. Binding sites were defined as the 200-bp genomic region centered at the binding-peak summit. Coincident PIF-binding sites were defined as those that overlapped by at least 1 bp. By these criteria, we identified 1136 PIF1 binding sites that overlapped with the PIF4 binding sites (see overlapping Venn sectors in Figure 1A). We also included in our analysis 1064 PIF3 binding sites recently identified in etiolated seedlings (Zhang et al., 2013), as well as 2058 PIF5 binding sites, which, for uniformity, were derived from reanalysis of the ChIP-seq data of Hornitschek et al. (2012), using our present criteria. These authors used 10-day-old light-grown seedlings that were shade-treated for 2 h. This analysis identified 373 genomic regions that show overlapping binding sites for all four PIFs (Figure 1A).

G-Box and PBE-Box Motifs Together Dominate PIF1 and PIF4 Binding Sites

We performed a *de novo* motif discovery on the PIF1 and PIF4 binding sites using MEME software (Bailey et al., 2006) and identified the previously described G-box and PBE-box motifs (Hornitschek et al., 2012; Oh et al., 2012; Zhang et al., 2013) as statistically over-represented within both data sets (Figure 1B). The majority of PIF1 (62%) and PIF4 (54%) binding sites contained either one or both motifs (Supplemental Table 1 and Figure 1C). The subset of binding sites that displayed binding by all four PIFs showed the highest enrichment (94%) with G-box, PBE-box, or both motifs. When we searched for the nearest *cis*-element within a 2-kb window surrounding the combined genomic regions bound by PIF1, PIF3, PIF4, or PIF5, 68% of the G-box motifs and 46% of the PBE-box motifs were found to cluster within the 200-bp binding-site window (Figure 1D).

Direct binding of PIF1 to G-box and PBE-box containing probes was validated *in vitro* using Electrophoretic Mobility Shift Assays (EMSAs) (Figure 1E and Supplemental Figure 1A). PIF1 was found to bind directly to both G-box and PBE-box motifs as previously reported for PIF3 (Zhang et al., 2013) and PIF4 (Hornitschek et al., 2012; Oh et al., 2012). Additionally, several binding sites containing G- or PBE-boxes, or both, binding motifs were also tested for enrichment by ChIP-qPCR, in order to validate our ChIP-seq results and to confirm the specific association of PIF1, PIF3, and PIF4 with the identified genomic regions (Supplemental Figure 1B).

Identification of Genes Bound by the PIF-Quartet Members

PIF-binding genes were defined as those having one or more G- or PBE-box-coincident PIF-binding peaks, within

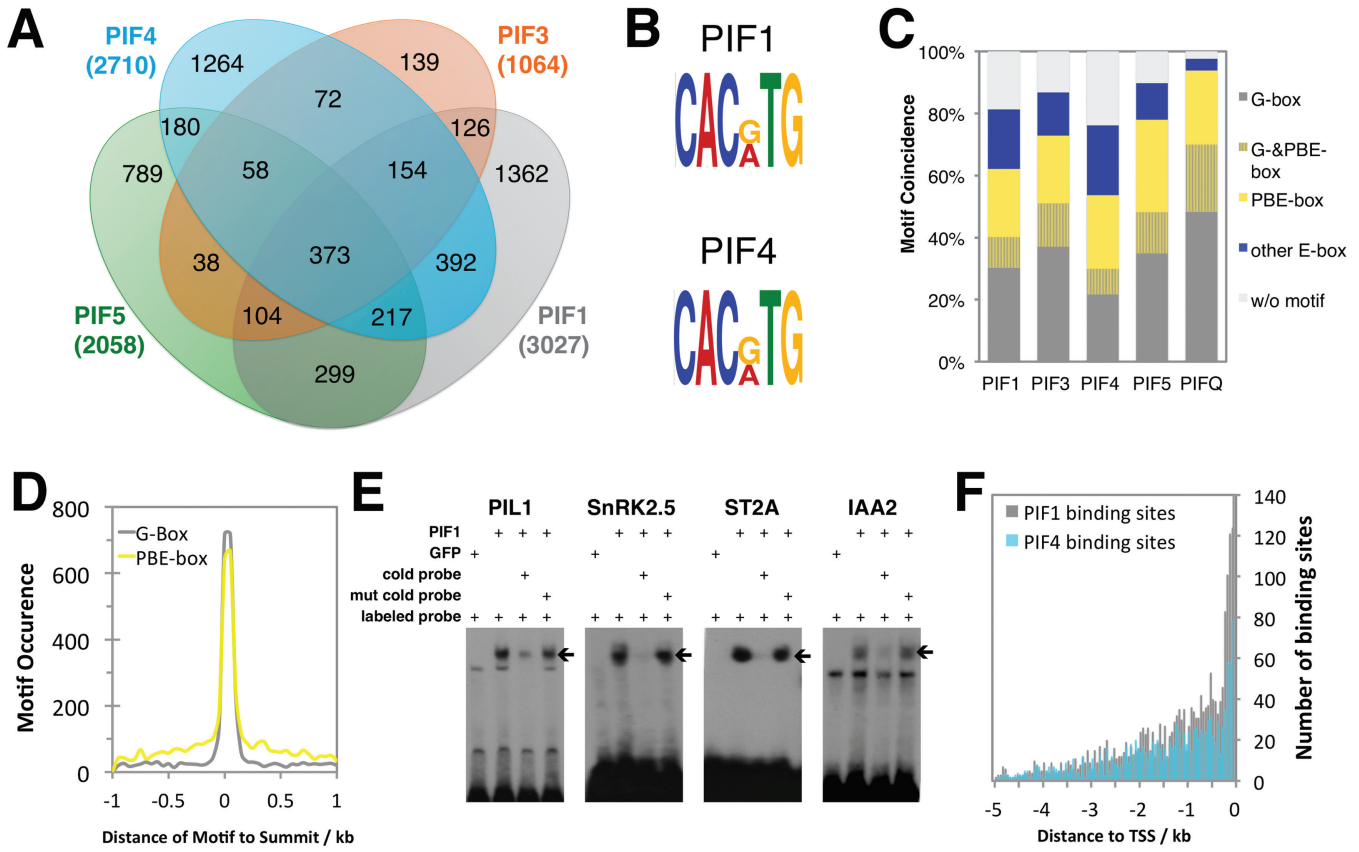

Figure 1 ChIP-Seq Analysis Identifies Shared and Separate Binding Sites for PIFs 1, 3, 4, and 5 Genome Wide.

(A) Venn diagram depicting total numbers (parentheses) and overlap of statistically significant, reproducible binding peaks for all four PIFs, genome-wide (Venn ovals), defined by ChIP-seq analysis. Genomic sites that bind from one to four different PIFs were identified.

(B) *De novo* motif discovery using MEME reveals that two dominant motifs, termed G-box (CACGTG) and PBE-box (CACATG), are enriched at PIF1 and PIF4 binding sites.

(C) Percentage of binding sites bound by the individual PIFs or all four PIFs (PIFQ) that coincide with G-box and/or PBE-box motifs.

(D) Distribution of the first occurance of G- and PBE-box motifs as a function of distance from the peak summits of binding sites bound in common by all four PIFs.

(E) PIF1 binds *in vitro* to DNA probes containing either a G-box (*PIL1*, *SnRK2.5*, *ST2A*) or a PBE-box (*IAA2*), as determined by EMSA assay. mut cold probe, mutated unlabeled probe.

(F) Distance to the next transcription start site (TSS) from PIF1- and PIF4-binding sites.

5 kb upstream of their transcription start sites (TSS), in an intergenic region (i.e. with no intervening gene between the binding site and the TSS) (Zhang et al., 2013). G- and PBE-box coincidence was selected because of the experimentally established sequence-specificity of the binding of the PIFs to these motifs (Hornitschek et al., 2012; Oh et al., 2012; Zhang et al., 2013; Figure 1E and Supplemental Figure 1A and 1B). By these criteria, PIF-associated genes were, in some cases, identified as having more than one binding site, and individual binding sites were found that are associated with up to two genes on opposite DNA strands. Our lists comprise 1911 genes associated with 1493 binding sites for PIF1, 828 genes bound by PIF3 at 596 sites (Zhang et al., 2013), 1279 genes bound by PIF4 at 1012 binding sites, and 1185 PIF5-binding sites (redefined from the data of Hornitschek et al., 2012) associated with 1497 genes (Supplemental Table 2). Eighty-eight percent of the PIF1 binding sites, and 86% of the PIF4 sites, were less than 3 kb away from the nearest TSS, respectively (Figure 1F).

PIF1, PIF3, PIF4, and PIF5 Collectively Regulate Gene Expression during Skotomorphogenesis

To define the contribution of the individual PIFs to the regulation of gene expression during skotomorphogenesis, we performed RNA-seq analysis on 2-day-old etiolated seedlings

of 10 different genotypes, including WT, *pifq*, the four single *pif*-mutants, and the four possible triple *pif*-mutant combinations. For each of the four PIFs, we conducted a gain-of-function (e.g. *pif3pif4pif5* versus *pifq* for PIF1) and loss-of-function (e.g. *pif1* versus WT) comparison to identify genes displaying Statistically-Significant Two-Fold (SSTF) expression changes between these genotypes, as previously described (Zhang et al., 2013). In addition, genes showing SSTF expression changes in the *pifq* versus WT comparison defined the baseline gene set collectively regulated by the PIF quartet (Supplemental Table 3). This set contains 2860 genes. A proportional three-way Venn diagram depicting the overlap between the gain-of-function, loss-of-function, and PIF-quartet-regulated gene sets for each individual PIF is shown in Figure 2A. Figure 2B shows the separation of *pif*-mutant up-regulated from *pif*-mutant down-regulated genes for each PIF in this comparison. A subset of genes displayed a direction of regulation (induction or repression) by an individual PIF that was contrary to the direction of regulation supported by the PIF quartet (e.g. expression induced by PIF1, but repressed by the PIF quartet) (46 genes for PIF1, 15 for PIF3, 38 for PIF4, and 130 for PIF5). These genes were excluded from the Venn sectors shown in Figure 2 and from further analysis. Consequently, the number of genes designated as PIF-quartet-regulated in Figure 2 is less than 2860 and varies for the individual PIF comparisons.

Subsequently, the loss-of-PIF-function and gain-of-PIF-function gene sets for each PIF in Figure 2 were merged into a single set (called a 'composite' gene set), which thereby defined the total number of PIF-regulated genes for each individual PIF, separately. By this analysis, PIF1 regulates 1996 genes, PIF3 regulates 405 genes, PIF4 regulates 708 genes, and PIF5 regulates 579 genes, compared to 2860 genes regulated collectively by the PIF quartet, as determined by the *pifq* versus WT comparison (Supplemental Table 3). The overlap among these data sets depicted in Figure 3 shows that, of the collectively PIF-quartet-regulated genes, PIF1 alone regulates 1117 (39%), PIF3 alone regulates 211 (7%), PIF4 alone regulates 501 (18%), and PIF5 alone regulates 192 (7%). The reason for the lack of PIF-quartet regulation of a subset of genes that are apparently regulated by individual PIFs is unknown and was not pursued further here. Conversely, however, the collective regulation of a considerable number of genes by the PIF quartet in the apparent absence of significant regulation by the individual PIFs alone is suggestive of a substantial level of redundant and/or cooperative regulatory activity among these four transcription factors (Figures 2 and 3).

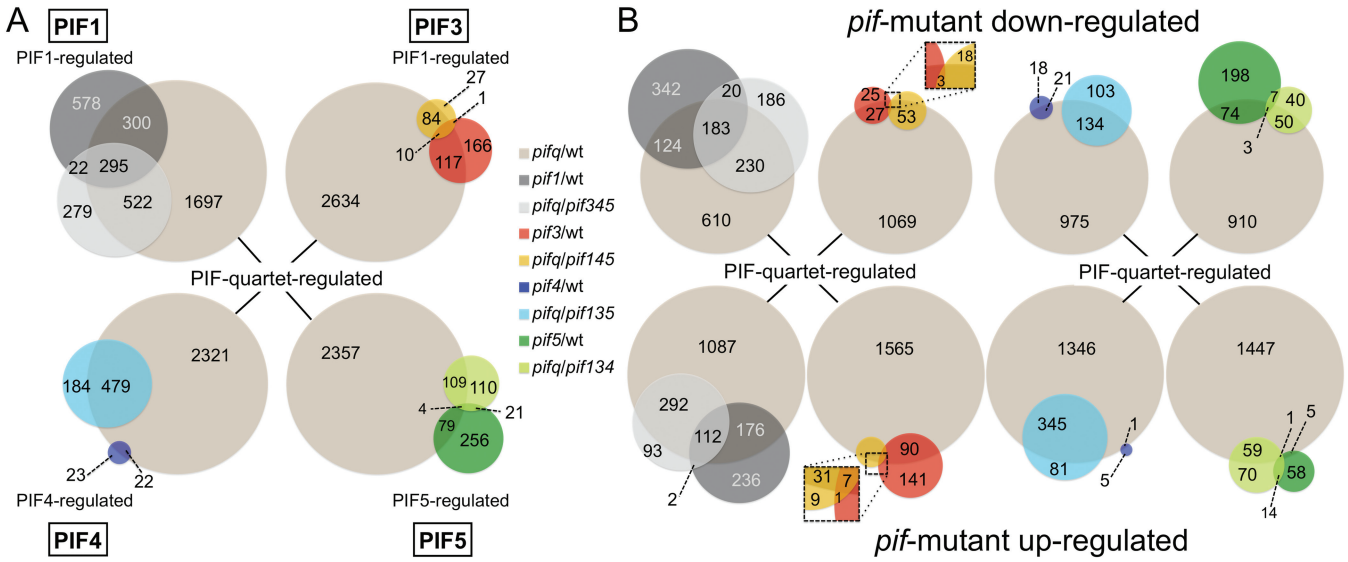

Figure 2 RNA-Seq Analysis of Selected *pif*-Mutant Combinations Identifies Genes Regulated Differentially by the Individual PIFs Genome-Wide.

(A) Venn diagrams depicting the gene numbers regulated by each individual PIF, the genes collectively regulated by the PIF quartet, and the genes in common (overlapping sectors). The genes in each Venn circle were identified as displaying Statistically Significant Two-Fold (SSTF) differences in expression in the pairwise genotypic comparisons shown in the legend. Genes displaying a mechanistically inverse direction of SSTF regulation in the WT/*pif* (loss-of-function) and *pif*-triple-mutant/*pifq* (gain-of-function) comparisons (e.g. deduced PIF-quartet and PIF1 promotion in the WT/*pifq* and WT/*pif1* comparisons, respectively, but deduced PIF1 repression in the corresponding *pif3pif4pif5*/*pifq* comparison) were excluded from the analysis shown here.

(B) Separation of genes into *pif*-mutant down-regulated (upper row) and *pif*-mutant up-regulated (lower row). This separation is based on the direction of the change in expression displayed in each pairwise genotypic comparison.

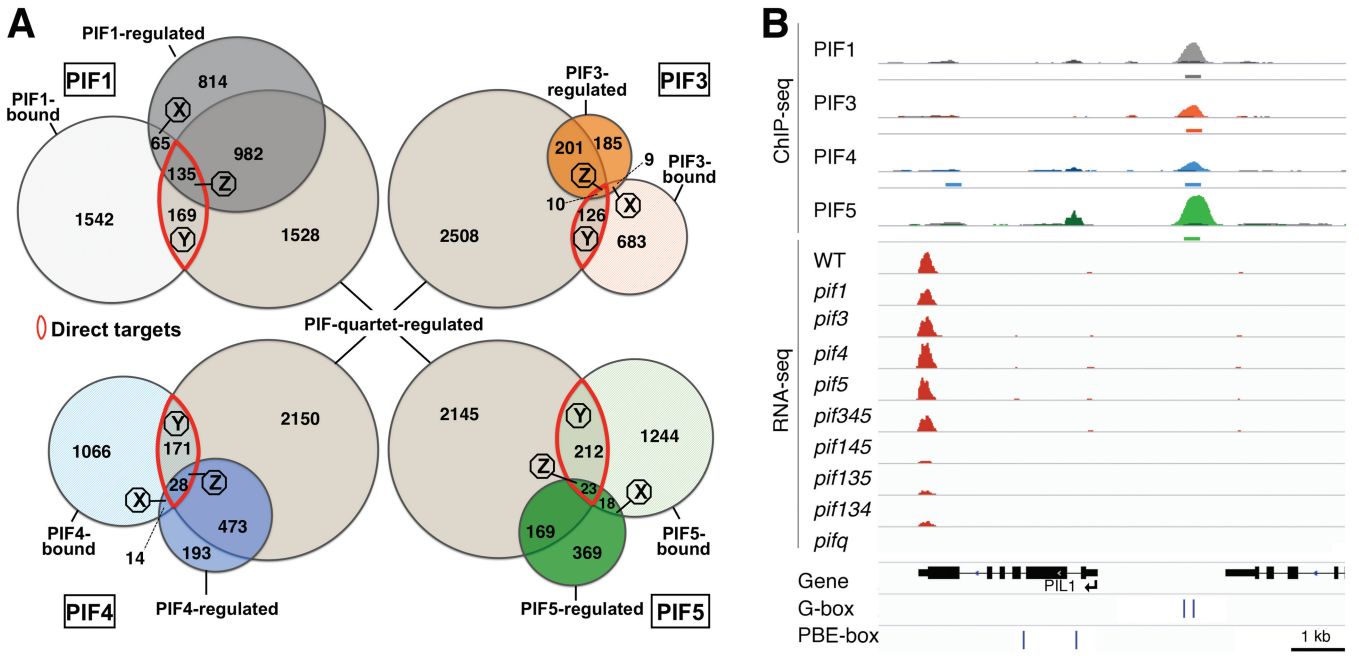

Figure 3 Integration of ChIP-Seq and RNA-Seq Data Sets Identifies Potential Direct Targets of PIF1, PIF3, PIF4, and/or PIF5 Transcriptional Regulation.

(A) Venn diagrams showing the overlap of genes displaying promoter-localized, G-, or PBE-box-coincident, PIF-binding peaks (PIF-bound genes), with those displaying PIF-quartet- and/or individual PIF-regulated expression (as defined in Figure 2A). This comparison defines seven classes of genes corresponding to the diagram sectors. The number of genes in each class is indicated, and the three sectors that overlap the PIF-bound genes are labeled X, Y, and Z. Red crescents identify the Y- and Z-class genes.

(B) Visualization of ChIP-seq (upper tracks) and RNA-seq (lower tracks) data for the genomic region surrounding the *PIL1* locus. The ChIP-seq tracks show the pile-up of all the reads obtained from MACS analysis of the data set from each experiment (color-coded for each PIF). The data for each corresponding WT-ChIP/input control are overlaid in dark gray. MACS-identified binding sites are indicated by the colored bar below the pile-up tracks (extended to 200 bp around the centered peak summit defined as the binding-peak maximum). RNA-seq tracks show the pile-up distribution of the combined raw reads of three biological replicates for each genotype. G- and PBE-box: vertical lines indicate motif positions.

Potential Direct-Target Genes of PIF1, PIF3, PIF4, and PIF5 Identified by Merging ChIP-Seq and RNA-Seq Data Sets

By integrating the above ChIP-seq and RNA-seq analyses, we identified those genes that are likely direct targets of transcriptional regulation by each individual PIF and those that display apparent redundant regulation by multiple PIF-quartet members (Supplemental Table 3). Direct-target genes of an individual PIF are defined here as those that are concurrently both bound and regulated by that PIF. The Venn diagrams in Figure 3A show, for each PIF independently, the overlap of the genes identified as displaying SSTF, PIF-quartet-, and/or individual PIF-regulated expression, with those genes showing promoter-localized, G-, or PBE-box-coincident binding of that PIF. Visualization in gene-browser format of an example of the data used in this analysis is depicted for the *PIL1* gene in Figure 3B. This gene displays both binding of all four PIF-quartet members to a site containing three G-box motifs in its promoter, and promotion of expression by each of the individual PIFs in the absence of the other three.

The central sector of each Venn diagram in Figure 3A (labeled Z) represents those genes that we define as high-confidence direct targets of the relevant individual PIF-quartet member (designated Class Z genes (Supplemental Table 3); see Zhang et al., 2013), as these display concurrent promoter-localized binding and SSTF transcriptional regulation by that PIF. However, we also included the genes in sector Y of each of the Venn diagrams as potential direct targets of the relevant individual PIF, in our further analysis (Supplemental Table 3), for the following reasons. Previously, we found for PIF3 that a substantial fraction of genes that display PIF3 binding, but less than two-fold PIF3-regulated changes in expression by RNA-seq analysis, still showed statistically significant changes in expression at more moderate levels, by qPCR analysis (Zhang et al.,

2013). In addition, the absolute contribution of an individual PIF-quartet member to the total expression difference between the WT and *pifq* mutant, in our experimental design, could readily be less than two-fold the absolute *pifq*-mutant expression level, if the four PIFs are contributing additively to the difference. For example, if all four PIFs were contributing equally additively to the *pifq*–WT difference, a minimum five-fold difference between WT and *pifq* would be necessary for any given PIF to reach the two-fold difference above or below the *pifq* level. Although *PIL1* does display a WT–*pifq* mutant differential in excess of five-fold (Figure 3B), the majority of SSTF genes do not. Thus we defined a composite class of genes designated Y+Z for each PIF as being potential direct targets of transcriptional regulation by that PIF (Supplemental Table 3). Interestingly, this subset of genes represents an equivalent proportion (16%) of the total genes bound by each of the PIFs, respectively (Figure 3A).

In total, 423 Y+Z genes were identified by these criteria as potential targets of one or more PIFs. Of these, 72% (304 genes) were bound and potentially regulated by PIF1, 32% (136 genes) by PIF3, 47% (198 genes) by PIF4, and 56% (236 genes) by PIF5. The overlap among these four gene sets is displayed in the Venn diagram in Figure 4A. The data show that more than half of the genes are bound and potentially regulated by more than one PIF (55%, 234 genes), with 20% (83 genes) being potential direct targets of all four quartet members. Conversely, a total of 189 genes (45%) display binding and potential regulation by only a single PIF protein (PIF1, 87 genes (21%); PIF3, 11 genes (3%); PIF4, 32 genes (8%); and PIF5, 59 genes (14%)) by these criteria.

Consistently with the established role of the PIFs as transcriptional activators in etiolated seedlings (Huq et al., 2004; Al-Sady et al., 2008; de Lucas et al., 2008; Shen et al., 2008; Hornitschek et al., 2009), the majority of these potential direct-target genes (62%, 262 genes) were induced by one or more PIFs (i.e. were down-regulated in the *pif* mutant(s)) (Figure 2B). These genes are therefore designated here as 'PIF-induced' (Zhang et al., 2013). Conversely, genes displaying up-regulation in the *pif* mutants (Figure 2B) are designated as 'PIF-repressed'. The bar graphs in Figure 4B depict the average expression level of all PIF-induced and PIF-repressed potential target genes, respectively, relative to WT in the *pifq* and triple mutant genotypes. As indicated above, if each of the four PIFs was to contribute additively and equally to the expression difference between the *pifq* mutant and WT, each PIF would contribute 25% to the total expression change observed in the mutant. The data show, however, that, on average for the PIF-induced genes, PIFs 3, 4, and 5 promote expression about equally to a level slightly less than 25% (18%–23%), whereas PIF1 acts considerably more robustly, promoting expression by about 65% on average (Figure 4B).

To visualize the relative contribution of each PIF to the regulated expression of the individual genes identified in Figure 4A and 4B, we arrayed the percent-contribution values in descending rank order for the induced and repressed genes separately (Figure 4C). Most of the PIF-induced and -repressed genes (76% and 83%, respectively) show a contribution of PIF1 to the regulation exceeding the 25% level. The other three PIFs exceed this level for only 34%–38% of all induced potential direct-target genes, and 44%–60% of the repressed ones. We defined individual genes displaying responsiveness to a given PIF that was less than the 25% threshold as having minimal responsiveness to that PIF, implying, conversely, that one or more other PIFs have a quantitatively more dominant or selective role in regulating that gene. The Y-class genes displaying such minimal responsiveness to a given PIF were eliminated as nominal direct targets of that particular PIF for the purposes of further analysis here. On this basis, 85 genes were excluded, leaving a total of 338 (209 (62%) PIF-induced and 129 (38%) PIF-repressed) on our 'final list' of genes that are proposed direct targets of transcriptional regulation by one or more PIF-quartet members (Supplemental Tables 4–6).

Figure 4D shows that overall there is a reasonable degree of correlation between the level of expression promoted by the collective activity of the PIF quartet (as determined by the difference in the RNA-seq reads of the WT and *pifq* genotypes) in the PIF-induced genes of this 'final list' and the sum of the levels of expression promoted by each PIF individually (as determined by the sum of the differences in RNA-seq reads between the respective *pif*-triple mutants and the quadruple *pifq* mutant). This observation suggests that the four PIFs tend to act more or less additively in promoting the expression of these direct-target genes, although there are clearly a number of individual genes that deviate significantly from this pattern.

Different PIFs Regulate Different Target Genes Differently

The central constellation of Figure 5 summarizes the distribution of the 338 'final list' genes across the 14 possible combinatorial categories of PIF-quartet-regulated expression derived from the above analysis. The surrounding bar graphs in this figure depict the average expression levels in the quadruple and four triple *pif* mutants, relative to WT, for the target genes in each individual category, separated into PIF-induced and PIF-repressed genes. More than one-third of these targets (128 genes) were concurrently bound and regulated by more than one PIF, and 11 genes were found to display convergent binding and regulation by all 4 PIFs. The reason for the substantial decrease in the number of genes designated as direct targets of all four quartet members in Figure 4A to that shown in Figure 5 is

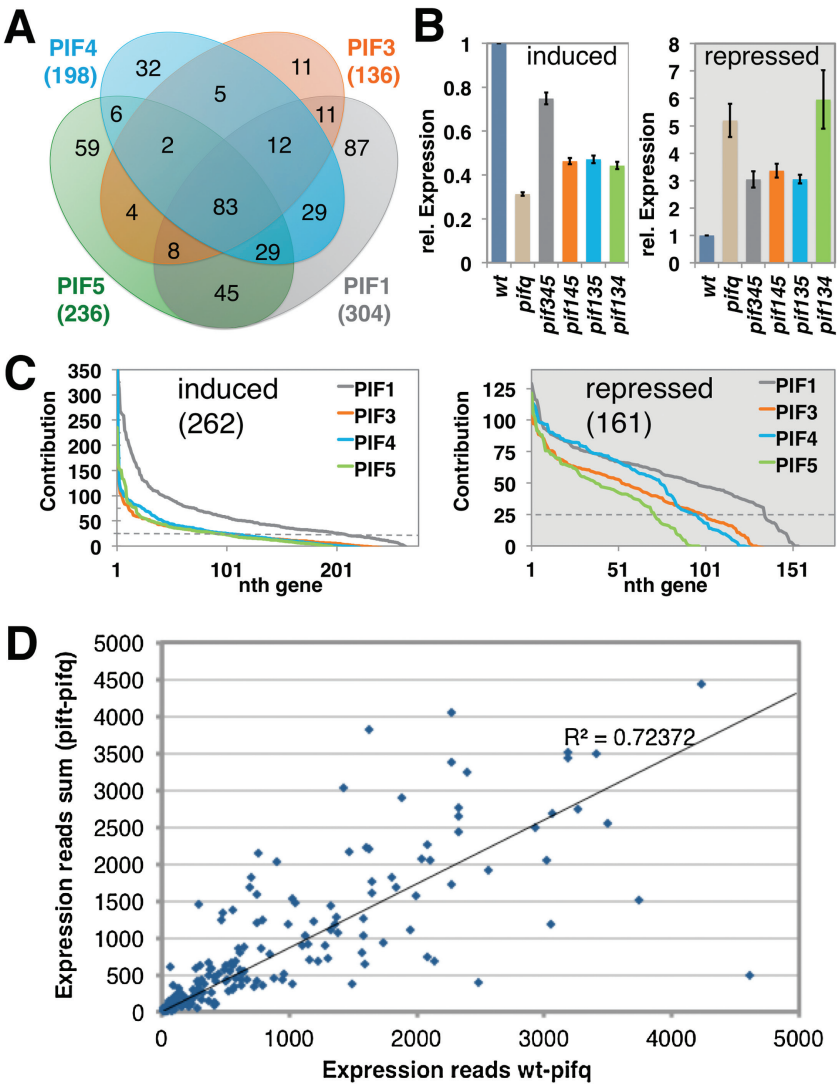

Figure 4 PIF-Direct-Target Gene Sets Display Varying Degrees of Overlap.

(A) Venn diagram depicting the overlap between the Y- and Z-class genes (combined) defined as potential direct targets of regulation by each individual PIF in Figure 3A.

(B) Average expression for each *pif*-mutant combination relative to wild-type (WT) summarized for the genes depicted in (A) after separation into PIF-induced (i.e. *pif*-mutant down-regulated) and PIF-repressed genes (i.e. *pif*-mutant up-regulated). Genes showing expression changes of more than 100-fold were excluded.

(C) Contribution of the individual PIFs in the absence of the other three (measured as the expression difference between the corresponding *pif*-triple (*pift*) and *pifq* mutant (PIF gain-of-function configuration)) to the collective regulation by all four PIFs (measured as the expression difference between the WT and *pifq*) (Zhang et al., 2013). All genes shown in (A) are arranged in descending rank order based on their contribution value for each individual PIF. The horizontal dashed line indicates a 25% contribution.

(D) Scatter plot showing correlation for individual genes between the expression difference between WT and *pifq* mutant (Expression reads (wt-pifq)) and the sum of the expression differences between each *pif*-triple mutant and *pifq* for all four PIFs (Expression reads sum (pift-pifq)).

that the imposed 25% threshold removed one or more PIFs from that category, thus lowering the number of quartet contributors for many genes. From this analysis, PIF1 is the dominant quartet member, directly targeting two-thirds of the entire target-gene set. Of these, 137 genes (41% of the targets) show single PIF concurrent binding and regulation by PIF1 alone. On the other hand, the contributions of the other PIFs, and the diversity of response patterns elicited by the different quartet combinations, are apparent across the different gene sets (Figure 5, bar graphs).

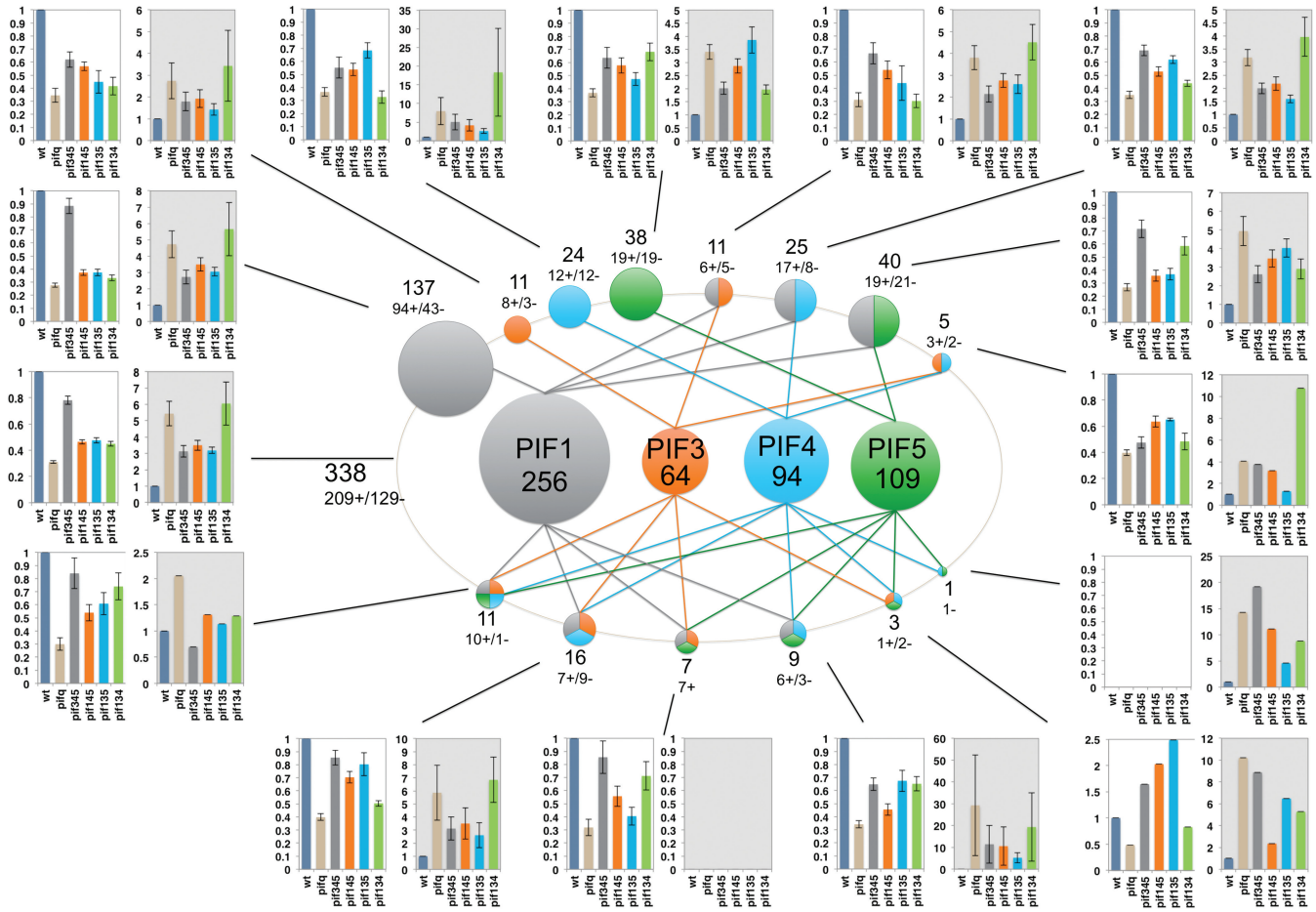

Figure 5 Classification of PIF Target Genes Based on Their Concurrent Regulation and Binding by Individual PIFs.

The four center circles display the number of target genes identified for each individual PIF. The outer circles depict the classification of target genes according to the PIFs that bind to and regulate them. Genes in all possible combinatorial categories are represented, ranging from a single PIF to all four quartet members. Numbers represent the total number of genes per class (top), subdivided into PIF-induced (+) and PIF-repressed (–) genes (bottom). Surrounding bar graphs depict the average expression of induced ('+', white background) and repressed ('–', gray background) genes of each individual target-gene class. Genes showing expression changes of more than 100-fold were excluded from the mean expression charts (four genes).

This diversity of differential regulation of the identified target genes by the individual PIFs becomes even more apparent when the relative contributions of the individual PIFs to the expression of the individual genes are arrayed three-dimensionally. Figure 6A displays representative segments of these arrays for the PIF-induced direct targets of each of the PIF combinations (see Supplemental Figure 2A–2E for the full arrays and Supplemental Table 5 for the gene lists). The PIF-quartet members vary in the extent of their contribution to the regulation of any given individual gene, and each individual PIF varies in its contribution to the regulation of different genes. Overall, this results in a complex regulatory pattern, in most cases involving more than one member of the quartet.

The data show that many of the target genes nominally categorized by our criteria as concurrently bound and regulated by only a single PIF also display some level of contribution from one or more of the other PIFs to their regulation. This observation indicates that, although a given single PIF apparently selectively or dominantly regulates these direct-target genes, other quartet members frequently supplement this activity to a greater or lesser extent. This outcome could be due to the categorization thresholds (SSTF and 25% contribution) used in our analysis, the limits of quantitative resolution provided by ChIP-seq and RNA-seq data, or other non-binding quartet members acting indirectly on those target genes. Nevertheless, conversely, as indicated above, 128 of our final list of target genes (76 induced and 52 repressed) show convergent binding and regulation by two or more PIFs, based on our analytical criteria.

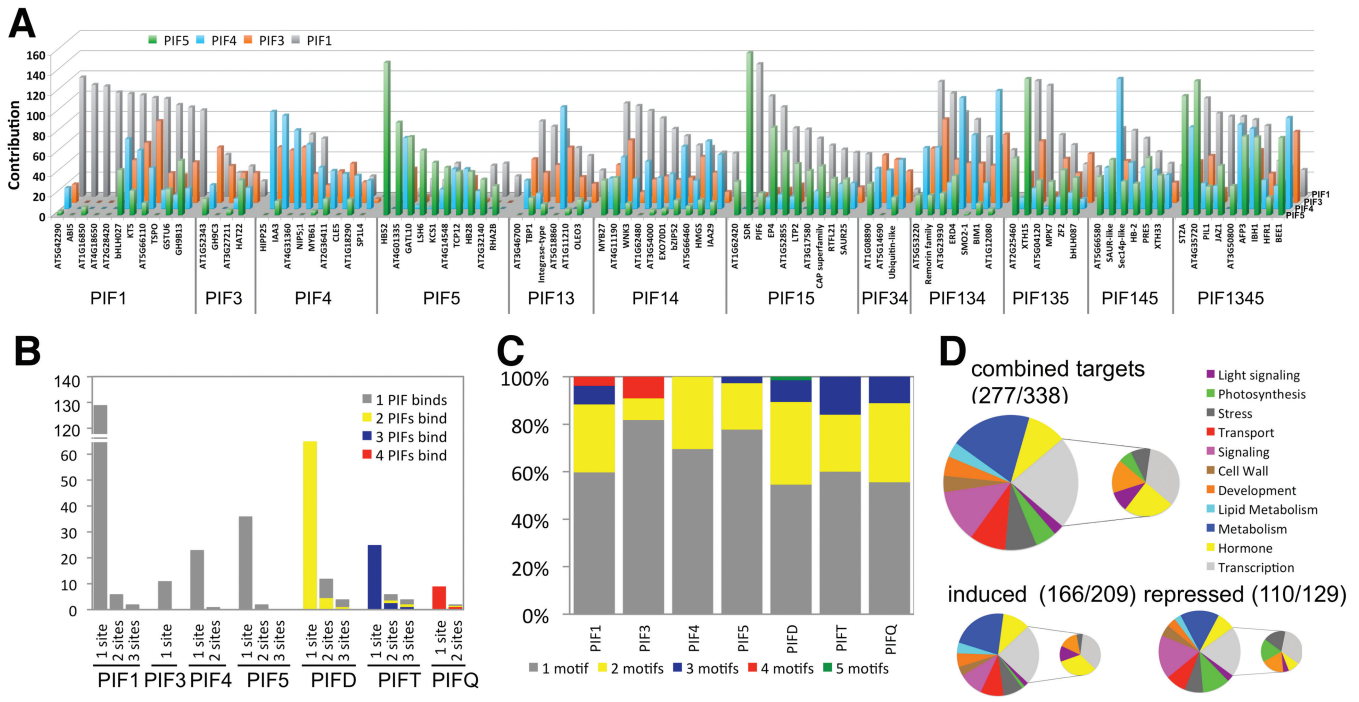

Figure 6 Differential Direct-Target Gene Regulation and Functional Classification.

(A) The different PIFs regulate different genes differently. The contribution of each PIF to the expression of selected direct-target genes in the different classes defined in Figure 5 is shown. The full arrays for all genes in each class are shown in Supplemental Figure 2.

(B) Distribution of the number of binding sites and the corresponding number of binding PIFs per promoter for each gene class.

(C) Distribution of the number of motifs per single binding sites of 200-bp length for each gene class.

(D) Functional categorization of all 'Final list' direct-target genes. (Top) The final target genes were assigned to functional categories, color-coded as shown. This assignment was based on the Gene Ontology annotations for biological and/or molecular function in the TAIR database. The percentage of the total annotated genes within each category was calculated after excluding the genes annotated as having unknown function. (Bottom) PIF-induced and PIF-repressed genes were assigned separately to the functional categories as described in (Top).

To assess the reliability of the above RNA-seq-based categorization of the quantitative contributions of the individual PIFs to the total quartet activation of induced direct-target genes, we performed RT–qPCR analysis of 33 selected representative PIF-induced genes across the spectrum of defined categories (Supplemental Figure 3). The data show robust to moderate validation of the defined expression pattern for 22 (67%) of these genes, with the remainder showing weaker or minimal correlations. In a considerable number of cases, genes showing individual PIF contributions of <25% to the total sum quartet activity still display statistically significant increases in expression above the *pifq*-mutant level for that PIF by RT–qPCR. This suggests that the number of genes for which multiple PIFs contribute to transcriptional activation, at least partially, may be underestimated by imposition of this threshold in our filtering criteria. Visual inspection of the RNA-seq and associated ChIP-seq data support these conclusions, as shown for a selected subset of these genes in Supplemental Figure 4.

Dissecting the Architecture of PIF-Quartet-Target-Promoter Interactions

To begin to define the molecular basis for this apparent quantitatively differential co-regulation of individual genes by the multiple PIF-quartet members, we examined the architecture of the PIF-binding sites in the promoter regions of the target genes and the corresponding PIF-binding pattern. For this purpose, we determined the number of PIF-binding sites (peaks) per promoter, and the number of G-box and/or PBE-box binding motifs associated with each binding site, for each direct-target-gene promoter (Figure 6B and 6C). The data reveal a variety of different configurations across these promoters. The number of PIF-binding sites per promoter ranges from 1 to 3, with the majority (88%) having a single site, 9% having two sites, and the remainder three sites (Supplemental Tables 4 and 5). The binding patterns of individual PIFs similarly range from one to multiple sites within a given target promoter and, conversely, individual single-binding-site promoters

display binding of from one to four members of the PIF quartet (Figure 3B and Supplemental Figure 4). Although the binding of multiple PIFs to a single binding site within a promoter would initially suggest direct binding redundancy, the issue is more complex because of the frequent occurrence of multiple G-box and/or PBE-box motifs within single PIF-binding peaks. Of the 179 lone binding sites in the promoters of the PIF-induced gene set, 102 (57%) have a single motif, 55 (31%) two motifs and 22 (12%) three or four motifs (Supplemental Tables 4 and 5).

Integration of these data with the composite PIF-binding and -regulation patterns provides the opportunity, at the one extreme, to identify single motifs that support selective or dominant transcriptional activation of a single gene, by one or other single PIF-quartet member, and, at the other, to define single motifs that support apparently shared transcriptional activation of a single gene, by up to all four quartet members. This analysis shows that, of the 102 single-binding-site/single-motif, PIF-induced genes, 73 (72%) display selective binding and direct transcriptional activation by a single PIF (PIF1, 49 genes; PIF3, 6 genes; PIF4, 6 genes; PIF5, 12 genes), while the remaining 29 genes (28%) display varying degrees of shared binding and transcriptional activation, by combinations of two (19 genes), three (6 genes), or four (4 genes) quartet members (Supplemental Tables 4 and 5). Together with another seven genes having lone, two-, or three-motif-containing, promoter-located binding sites that are bound by three or all four PIFs, respectively, this makes a total of 36 genes (50% of the single-site genes targeted by two or more PIFs) that display evidence that two or more PIFs redundantly share a single motif in the target gene. Collectively, these data thus suggest a continuum of motif recognition ranging from strongly specific or selective to relatively equivalent by the four PIFs. Not unexpectedly, the genes with multiple PIF-binding sites in their promoters show additional complexity, as some of these sites also contain multiple motifs. The most striking example is *ATHB2*, which has five PIF-binding sites, containing nine motifs, in an extended 5-kb promoter, and displays shared transcriptional activation by PIF1, PIF4, and PIF5 (Supplemental Figure 4).

To examine whether the differential activities of the quartet members might be specified by the core G- and PBE-box motifs or their flanking sequences (Gordan et al., 2013), we conducted *de novo* motif discovery on the binding sites in the 338 direct-target promoters, using the MEME software (Bailey et al., 2006). This analysis revealed no additional motifs, besides the already described PBE- or G-boxes (Supplemental Figure 5). Nor could we identify any distinct signatures in the sequences flanking these known motifs that could account for this differential activity. Similarly, examination of the single motifs in the single binding sites of the 73 genes that show preferential binding of one PIF or another (PIF1, 49, genes; PIF3, 6 genes; PIF4, 6 genes; PIF5, 12 genes) showed no apparent differential preference for G- or PBE-boxes between the PIFs, nor was there evidence of specific extended motifs associated with differential binding of the individual PIFs (Gordan et al., 2013). Conversely, both G- and PBE-boxes were found capable of binding two or more PIFs in those 29 single-binding-site/single-motif promoters that are targets of multiple PIFs. The data thus reveal no obvious DNA-sequence-specified basis for any potential differences in binding affinity between the individual PIFs.

A number of factors could potentially influence the patterns of promoter binding and expression regulation displayed by the PIFs in our analysis. Differences in the spatial patterns of PIF expression could, in principle, support a diversity of target-gene expression patterns among the PIFs. To examine this possibility, we generated *Arabidopsis* lines transgenically expressing PIF-promoter::GUS constructs in our previous study (Zhang et al. 2013). The data show that all four PIF promoters support expression throughout all the organs and tissues of dark-grown-seedlings, with no distinctive differences in pattern detectable between the different PIFs (see Figure 6A–6D in Zhang et al., 2013). It seems unlikely, therefore, that organ- or tissue-specific differences in PIF expression can account for the diversity of target-gene expression patterns observed. The use of the CaMV 35S promoter to drive PIF expression for the ChIP-seq experiments has dual impact. On the one hand, it permits comparison of the DNA-binding patterns of the different PIFs in the presumptive absence of differences in expression patterns. On the other hand, it raises the possibility that the binding patterns observed will not reflect those of the endogenous proteins, because of differences between the spatial expression patterns of the *PIF* genes and the 35S-promoter-driven construct. Again this does not appear likely, as our data show that the expression pattern of a transgenically expressed 35S::GUS construct closely resembles that of the PIF-promoter::GUS constructs referred to above (see Figure 6A–6E in Zhang et al., 2013). Similarly, although there are differences in the levels of *PIF* gene expression at the transcript level, these do not correleate with the diversity of binding or expression patterns observed (see Figure 6D in Zhang et al., 2013). Although we do not have quantitative estimates of the comparative levels of the endogenous and transgenic PIF proteins, it is likely that the transgenic PIFs are higher than the endogenous proteins. This has the potential to distort the ChIP-seq-derived binding patterns by increasing the number of lower affinity interactions detected. However, our definition here of functionally relevant binding sites as those that are both coincident with G- or PBE-box sequence motifs and localized to the promoters of experimentally identified, PIF-regulated genes reduces the likelihood that this issue contributes to the broad diversity of different between-PIF-binding patterns that we observe. Our use of published PIF5 ChIP-seq data from another laboratory that used shade-treated,

light-grown seedlings (Hornitschek et al., 2012) means that these data (although reanalyzed using our computational procedures) are not directly comparable to those of the other three PIFs analyzed here, and do not directly parallel our RNA-seq identification of PIF5-regulated genes in the present study. On the other hand, there is evidence that shade treatment of green seedlings causes partial reversion toward the transcriptional pattern of dark-grown seedlings (Leivar et al., 2012), indicating at least partial overlap between these two physiological states. Consequently, it appears reasonable to conclude that genes that are both regulated by PIF5 in the dark, and bind PIF5 to a promoter-localized, G-, or PBE-box in the shade are strong candidates for being direct targets of PIF5 transcriptional regulation in dark-grown seedlings. Consistently with this conclusion, 73% of the PIF5-induced genes identified here by these combined criteria are also direct targets of (i.e. bound and regulated by) one or more of the other PIF-quartet members (Supplemental Table 5).

The Pattern of PIF–Genome Interaction Defines a Continuum of Promoter Occupancy and a Superimposed Local Modulation of Intrinsic Transcriptional Activation Potential

To determine whether there is a quantifiable relationship between the level of promoter-localized PIF binding and the consequent level of expression of the target gene induced by the bound PIF species, we compared the level of PIF-binding (as determined by ChIP-seq analysis) and PIF-induced expression (as determined by RNA-seq analysis) for each target gene, genome-wide. Initially, as a baseline, we examined the overall correlation between the combined total binding of all four PIFs to each promoter, and the level of expression of the corresponding direct-target genes, induced by the collective activity of the four quartet members. Although the slope of the regression line of the scatter-plot data in Supplemental Figure 6 suggests a generally positive relationship, the low R^2 value indicates the absence of a robust correlation between collective promoter-localized PIF occupancy and PIF-induced expression level.

To examine more specifically whether the variable contribution of each individual PIF to the total PIF-quartet-induced expression of each target gene, described above (Figures 5 and 6A), is quantitatively related to the level of promoter-localized binding of the relevant PIF species to each target gene, we performed a correlation analysis for each individual PIF. For this purpose, we defined the contribution of each PIF to the total binding activity of all four PIFs at each peak, as the percentage contributed by each individual PIF to the combined total PIF-quartet ChIP-seq reads. For multi-binding-site promoters, the respective ChIP-seq reads were summed across all peaks to provide a single contribution value for the promoter. In each case, this value was then compared with the relative contribution (percent) of the relevant individual PIF to the total expression level of the corresponding target gene, induced collectively by all four PIFs, as determined by the RNA-seq analysis described in Figures 5 and 6A.

This analysis is shown and discussed in detail in Supplementary Analysis 1 and Supplemental Figures 7–16. Overall, the fractional contributions of the individual PIFs to the collective promotion of target-gene expression by the four PIFs combined are poorly correlated with the corresponding respective levels of promoter occupancy by each PIF (Supplemental Figure 7). Subdivision of these direct-target genes into the multiple combinatorial categories of PIF regulation shown in Figure 5 likewise does not reveal any immediately obvious robust correlation between binding-site occupancy and expression promotion for each individual PIF (Supplemental Figures 8–12). This pattern is retained in the subset of genes having only one binding site with a single motif per promoter (Supplemental Figures 15 and 16), indicating that the lack of correlation is not simply the result of the complexity of having multiple binding sites per promoter and multiple motifs per binding site, as is true for a considerable fraction of the full gene set.

By contrast, examination of the 'PIF-binding' versus 'promoted-expression' profiles of the separate individual genes across the different combinatorial categories provides evidence of an intriguing pattern. For this analysis, the ChIP-seq reads for each individual PIF and the corresponding difference in RNA-seq reads between the *pifq* and relevant triple *pif* mutant (PIF-specific promoted expression) were plotted and subjected to linear regression analysis, separately for each individual target gene. The most striking result is displayed by the 31 genes in the combined triple- and quartet-targeted gene set, which show the highest levels of shared promoter occupancy and regulated expression by the PIF-quartet members. The data for the full gene set are arrayed in Supplemental Figure 17 and four selected representative genes from across the array are presented in Figure 7. There is a gradation in the trajectory of the relationship between occupancy level and promoted-expression level, from robustly positively correlated, through uncorrelated, to relatively robustly negatively correlated (Supplemental Figure 17). Moreover, because the levels of occupancy of PIF1 and PIF5 are almost invariably higher than those of PIF3 and PIF4, this inversion in the direction of the correlation is independent of the identity of the PIFs at the respective occupancy levels. For example, comparison of the converse patterns of *PHOSHOGLYCERATE MUTASE* (*PGM*) and *BEE1* at the two extremes of the array (Figure 7) shows that, for *PGM*, low-PIF4 and high-PIF1 occupancy result in low and high expression, respectively, whereas, for *BEE1*,

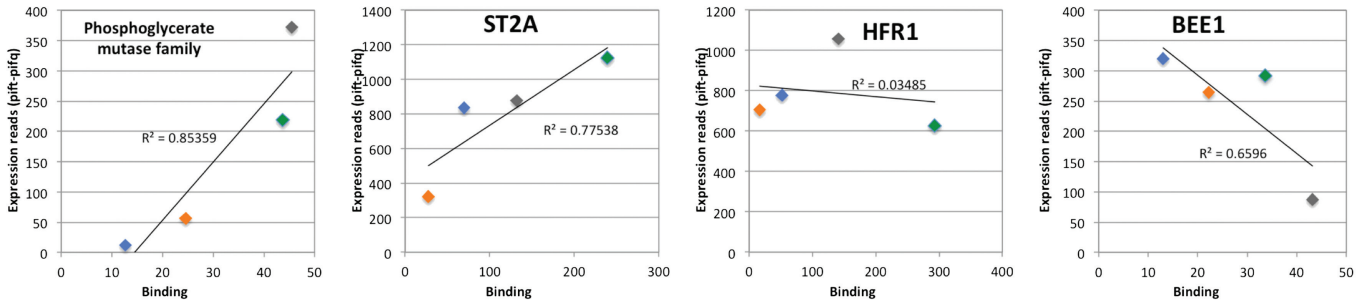

Figure 7 PIFs Display a Matrix of Variable Promoter Occupancy and Modulated Intrinsic Transcriptional Activation Activity toward Shared Direct-Target Genes.

Plots depict the relationship between promoter occupancy (Binding) by each PIF and the corresponding level of expression induced by that PIF (Expression reads [*pift-pifq*]) in four representative genes (*PGM*, *ST2A*, *HFR1*, and *BEE1*) from a graded array of 31 genes in Supplemental Figure 17. These 31 genes comprise all those defined here as shared direct targets of three or more members of the PIF quartet. Individual PIF-induced expression was determined by RNA-seq (normalized reads of *pifq* mutants were subtracted from reads of each triple *pif*-mutant (*pift*) line) and binding was determined as the PIF-specific ChIP-seq reads per promoter. Values for PIF1 are depicted in gray, for PIF3 in orange, for PIF4 in blue, and PIF5 in green.

low-PIF4 and high-PIF1 occupancy conversely result in high and low expression, respectively. *ST2A* is similar to *PGM*, whereas *HFR1* provides an example of relative independence of expression from occupancy level, on average. All four of these genes have single PIF-binding sites, each containing only a single motif (all G-boxes) in their promoters (Supplemental Tables 3–5). The data for the nominal PIF-dominant categories of genes, where a single PIF (PIF1, PIF3, PIF4, or PIF5, respectively) dominates promotion of expression relative to the other three, are generally consistent with this pattern (Supplemental Figures 18–22). Taken together, these data indicate that factors other than simple promoter or single binding-site occupancy level determine the fractional contribution of each PIF to the collective quartet activity, and that the influence of these factors varies from promoter to promoter for the different individual PIFs.

Functional Categories of PIF Target Genes

Categorization of our overall list of final direct-target genes, according to their known or predicted functions, reveals a strong enrichment for transcription-factor-encoding loci (Figure 6D), supporting the conclusion that the PIFs function as master regulators of a complex transcriptional network. A considerable proportion of the target genes also alternately indicate more direct regulation of a number of basic cellular functions in metabolism, transport, photosynthesis, and cell wall metabolism. As might be expected, photosynthesis-related genes display PIF repression, or lack of induction, in the dark-grown samples used, consistently with observed PIF function in repressing photomorphogenesis in etiolated seedlings. If this transcriptional repression is the direct consequence of PIF binding to those promoters, the data would indicate that the PIFs have dual molecular activity, concomitantly functioning as transcriptional activators and repressors of different genes.

Functional categorization of the subset of genes targeted by multiple PIFs shows an increased enrichment for genes involved in hormone signaling or hormone metabolism. Half of the analyzed target genes that show regulation through three or all four PIFs are either involved in regulation of transcription, plant hormone-associated functions, or both (Supplemental Figure 22). Examples include the transcription factors *PIL1*, *HFR1*, *BEE1*, *BIM1*, *IBH1*, *ATHB-2*, *PRE5*, *bHLH87*, and other genes like *JAZ1*, *HAI1*, and *ST2A*. However, examination of the specific genes regulated solely or predominantly by a single PIF did not reveal any evidence of PIF-specific regulation of any defined molecular or cellular pathways or processes. Thus there is no indication, at this level of resolution, of how PIF1 operates to be the dominant PIF controlling cotyledon separation (Leivar et al., 2012).

Comparison of the PIF-direct-target genes identified here with those previously determined to exhibit light regulation using microarray profiling (Leivar et al., 2009) shows that 38% of our final target genes exhibit PIF-dependent regulation that is reversed upon irradiation with red light. The majority of these (63%) are induced by the PIFs in the dark and repressed upon exposure to light (Supplemental Tables 4–6). Among these PIF-induced/light-repressed genes are several involved in auxin signaling, namely three SAUR genes and four ARF/IAA genes (*SHY2/IAA3*, *IAA19*, *IAA29*, and *ARF18*).

DISCUSSION

Numerous genome-wide transcription factor (TF)-binding studies have shown that TFs frequently bind to thousands

of DNA sites *in vivo* (Kininis et al., 2007; MacArthur et al., 2009; Ouyang et al., 2009; Sun et al., 2010; Ferrier et al., 2011; Li et al., 2011; Yu et al., 2011; Zhang et al., 2011; Cheng et al., 2012; Hornitschek et al., 2012; Oh et al., 2012; Tao et al., 2012; Chang et al., 2013; Zhang et al., 2013). As eloquently enunciated by Biggin (2011), these studies have led to the recognition that most TFs each bind to a majority of genes over a quantitative continuum of DNA occupancy levels, spanning functional, quasifunctional, and nonfunctional DNA-binding events (MacArthur et al., 2009; Cheng et al., 2012; Fisher et al., 2012). The accumulated data indicate that, in general, at one extreme, the hundreds of genes displaying the highest occupancy by a given TF are those most frequently its functionally significant targets. Conversely, at the other extreme, the thousands of genes displaying 10- to 100-fold lower occupancy levels of that factor are frequently not regulated to a degree that is biologically significant. The many genes in between these extremes display moderate binding and weak transcriptional regulation at levels (10% to two-fold) that are often of unresolved functional significance. Our strategy of imposing thresholds of transcriptional alteration for defining PIF-regulated expression established DNA-sequence-motif-coincidence for binding-site definition, and congruence of PIF-binding and expression alteration for defining functional occupancy was designed to focus on those genes deemed most likely to represent bona fide direct targets of PIF transcriptional regulation. Our focus on the PIF-induced genes here is based on the existing evidence that all four quartet members exhibit intrinsic, autonomous transcriptional activation activity (Huq et al., 2004; Al-Sady et al., 2008; de Lucas et al., 2008; Leivar et al., 2008; Shen et al., 2008; Hornitschek et al., 2009; Leivar and Quail, 2011; Zhang et al., 2013). Our analysis indicates that the pattern of PIF behavior in transcriptional activation of direct-target genes is generally consistent with Biggin's (2011) model, but is, in addition, overlain with another level of complexity that acts independently of occupancy level.

Previously, we showed by RT–qPCR that PIF1, PIF3, PIF4, and PIF5 contribute differentially to the combined PIF-quartet-promoted transcriptional activation of a small subset of 14 genes that are direct targets of PIF3 activation and discovered, surprisingly, that PIF1 dominates the level of activation of a considerable fraction of these genes (Zhang et al., 2013). Here we have additionally identified direct targets of PIF1 and PIF4 regulation and have provided evidence that this pattern of differential transcriptional activation by the quartet extends genome-wide, to over 200 genes that are apparent concomitant direct targets of one or more of the PIF-quartet members. Moreover, by dissecting the number and architecture of the promoter-localized PIF-binding sites and sequence motifs in the promoters of these genes, we have uncovered an array of variable TF–promoter configurations. Particularly notable are the substantial proportion of genes with multiple binding sites and/or multiple motifs per binding site in their promoters. In consequence, the transcription-factor–promoter configurations range from strongly preferential binding of single PIFs to lone binding sites containing single motifs in a single promoter, through binding of multiple PIFs to multiple multi-motif binding sites in a single promoter, to apparent cooccupation by all four quartet members of lone, single-motif binding sites in a single promoter. Although there is evidence that overall the quartet members tend to act additively to elicit the full induction of their direct-target genes (Figure 4D), examination of the binding and regulatory activities of each individual PIF toward its respective direct targets shows a poor correlation of these two molecular activities (Supplemental Figures 6–12, 15, and 16). These data indicate the absence of a simple quantitative relationship between the level of binding-site occupancy by each PIF and the corresponding level of transcription induced in the target gene by that PIF.

Interestingly, however, the correlative pattern revealed upon examination of each direct-target gene individually provides intriguing insight into the complexity of the molecular interface between these TFs and their target genes *in vivo*. For example, PIF1 has high transcriptional activation activity when bound at a high occupancy level at the single, shared binding motif in the *PGM* promoter (compared to the other PIFs), but has low transcriptional activation activity when bound at an equally high occupancy level at the single, shared binding motif in the *BEE1* promoter (compared to the other PIFs) (Figure 7 and Supplemental Figure 17). The exact converse is true of PIF4. This pattern indicates a matrix, defined by a quantitative continuum of binding-site occupancy by the PIFs, overlain by a level of locally imposed modulation of the intrinsic transcriptional activation potential of the individual occupying PIF at individual binding sites and, moreover, that both these regulatory parameters vary differentially between the individual PIF-quartet family members (Figure 7 and Supplemental Figure 17). As indicated in the 'Introduction' section, these parameters could include such factors as chromatin structure (e.g. histone or DNA modifications), transcriptional coregulators, cooperating or competing factors, and/or posttranslation-modifying enzymes (protein kinases, acetylases, etc.) (Kininis et al., 2007; Farnham, 2009; MacArthur et al., 2009; Li et al., 2011; Hahn and Young, 2011; Zhou and O'Shea, 2011; Lickwar et al., 2012). Intriguingly consistent with this general concept, there is recent evidence that PIF3 recruits a histone deacetylase, HDA15, to the promoters of some genes to suppress expression through local histone deacetylation (Liu et al., 2013).

While phy-controlled PIF abundance is clearly the overarching mechanism of light-repressed, and both shade- and diurnal-darkness-induced, PIF transcriptional activity (Monte et al., 2004; Bae and Choi, 2008; Moon et al., 2008; Leivar et al., 2009; Lorrain et al., 2009; Oh et al., 2009; Shin

et al., 2009; Leivar and Quail, 2011; Sentandreu et al., 2011; Hornitschek et al., 2012; Leivar et al., 2012; Li et al., 2012; Soy et al., 2012), there is increasing evidence in recent years that PIF activity is also modulated by a diversity of other endogenous (gibberellins (GA), brassinosteroids (BR), ethylene, circadian clock, sucrose) and environmentally induced (high temperature, photoperiod) signaling pathways. These effects are exerted at both transcriptional and posttranslational levels. *PIF4* and *PIF5* transcript levels have been shown to be circadianly regulated in light-grown plants (Nozue et al., 2007; Niwa et al., 2009), although those of *PIF3* are not (Soy et al., 2012). On the other hand, *PIF3* transcript levels are induced by ethylene, whereas those of PIF4 and PIF5 are not (Zhong et al., 2012). Exogenous sucrose has been reported to increase PIF5 protein abundance without affecting its transcript levels, suggesting carbon levels may regulate this response (Stewart et al., 2011). DELLA proteins have been shown to directly inhibit both PIF3 and PIF4 transcriptional activity by blocking DNA binding, and GA reverses this inhibition by inducing DELLA degradation (de Lucas et al., 2008; Feng et al., 2008). The BR-activated TF BZR1 has also been reported to form a DNA-bound bimolecular complex with PIF4 and coregulate common direct-target genes (Oh et al., 2012). Moreover, the DELLA proteins also interact with BZR1, inhibiting its DNA-binding capacity, similarly to PIF4 (Bai et al., 2012), suggestive of a three-way PIF4–DELLA–BZR1 regulatory complex. Elevated temperature has been reported to stimulate the binding of PIF4 to the promoters of two auxin-biosynthetic genes, leading to increased auxin levels and consequent enhanced cell-elongation rates (Koini et al., 2009; Lucyshyn and Wigge, 2009; Franklin et al., 2011). Collectively, these data indicate that the PIFs are the core of a transcriptionally centered signaling hub that provides a specific molecular mechanism for 'crosstalk' between multiple signaling and transcriptional networks (Castillon et al., 2007; Leivar and Quail, 2011).

In addition to the above-documented inter-pathway crosstalk, there is evidence and further potential for intra-family complexity among the PIFs themselves and other members of the *Arabidopsis* superfamily of bHLH TFs. HFR1, a non-DNA-binding member of the PIF-containing bHLH Subfamily 15 (Toledo-Ortiz et al., 2003), has been shown to inhibit the activities of PIF4 and PIF5 by forming non-DNA-binding heterodimers with them (Hornitschek et al., 2009). Similarly, PAR1, a member of a different group of HLH proteins, lacking a functional basic DNA-binding domain, similarly interacts with PIF4, inhibiting its DNA-binding activity (Roig-Villanova et al., 2006; Hao et al., 2012). Inter-PIF heterodimerization has been demonstrated for PIF3 and PIF4, with retention of sequence-specific G-box DNA binding *in vitro* by the heterodimer (Toledo-Ortiz et al., 2003). The potential for heterodimerization among all the different PIF-family members raises the possibility of yet more combinatorial complexity in DNA-binding-site recognition and transcriptional activity.

The morphological phenotypes of loss-of-function *pif* mutants have established that PIF1, PIF3, PIF4, and PIF5 act more or less additively, up to a saturation limit, to promote the skotomorphogenic development of dark-grown seedlings (Leivar et al., 2008; Shin et al., 2009; Leivar et al., 2012). The monogenic mutants of each PIF-quartet member display essentially no detectable visible phenotypic differences from WT, indicating almost complete redundancy. Double and triple mutants, on the other hand, show increasing degrees of partial photomorphogenic-like development in darkness, culminating in a *cop*-like phenotype in the quadruple *pifq* mutant that approaches that of light-grown WT seedlings. By contrast, in comparison to the *pifq* mutant, the four *pif*-triple mutants exhibit varying degrees of recovery of the etiolated phenotype, indicating that the individual PIFs have the autonomous capacity, to varying extents, in this gain-of-function configuration, to partially reactivate the transcriptional program that drives the skotomorphogenic developmental pathway. The differential activities of the individual PIF-quartet members are most particularly apparent for the cotyledon-separation facet of the deetiolation phenotype, where PIF1 strongly dominates the process, followed more or less equally by PIF4, PIF5, and PIF3 (Leivar et al., 2012).

The overall pattern of transcriptional regulation of direct-target genes by the PIF-quartet members, individually and collectively, is generally consistent with these morphological phenotypes. Most strikingly, PIF1 dominates the induction of many direct-target genes, genome-wide, confirming and expanding on our earlier RT–qPCR data for selected genes (Zhang et al., 2013). Our analysis also identifies a core set of 29 genes that are robust co-direct targets of transcriptional induction by three or all four quartet members (designated 'QT-genes'), demonstrating the existence of a high level of qualitative functional redundancy between these PIFs, in some cases through a single DNA-recognition motif, for at least a subset of these genes. The apparent general propensity of PIF1 to display higher average binding-site occupancy of direct-target genes than the other PIFs may be responsible for the larger PIF1-dominant gene set identified here than for the other PIFs. We did not detect any differences in binding-site or nearby promoter DNA sequences that might explain such occupancy differences, suggesting the possibility of a higher intrinsic affinity of PIF1 than of the other PIFs for these shared sites on average. However, although the measured transcript levels are similar (at least for PIF1, PIF3, and PIF4) (Supplemental Figure 14), we cannot rule out the possibility that higher PIF1 protein abundance contributed to this pattern.

Functional categorization of the 'final list' of direct-target genes shows strong enrichment of those encoding established or predicted TFs (Figure 6D and Supplemental Figure 22). The diversity of TF classes represented in this gene set implies broadly pleiotropic regulation of multiple branches of the downstream transcriptional network. This is most striking for the QT-gene subset, where 50% of the annotated targets encode TFs. This indicates a central role

of these genes in transducing light-activated phy signals to major sectors of the transcriptional cascade. The functions of some of these TFs in downstream processes have been investigated, including *PIL1*, *ATHB2*, and *HFR1* (shade-avoidance), *BIM1*, *BEE1*, *IBH1*, and *PRE5* (brassinosteroid signaling), and *JAZ1* (a transcriptional repressor of multiple TF classes, that was initially identified as a repressor of jasmonate (JA) signaling). In addition, however, the remaining genes in the other functional categories suggest that the PIFs also exert more direct control over other cellular pathways, not involving transcriptional regulation, including *PGM* (glycolysis/cellular energy production), *XTR7* and *XTH33* (cell wall growth), *MPK7* (MAP kinase signaling), *AFP3* (ABA signaling), and *ST2A* (JA signaling). Although there are no immediately obvious indications from the expression patterns of specific pathways preferentially regulated by PIF1 that would explain the dominance of this factor in suppressing cotyledon separation, the identified direct-target genes provide the opportunity for future genetic studies aimed at defining these pathways.

The present findings thus provide a framework for defining the molecular mechanisms by which closely related TFs, like the PIF quartet, exert both shared and strongly differential direct transcriptional control of target genes, and how this relates to the overlapping and distinct functions of the individual factors in regulating downstream morphogenic responses. More broadly, the multiple layers of complexity unveiled here are perhaps not surprising for a signaling hub that functions at the convergence of multiple, major, plant regulatory pathways, to distribute incoming signaling information to the appropriate downstream sectors of the transcriptional network. The challenge is to define whether and, if so, the molecular basis by which the PIFs discriminate between incoming signals of different origin, and how this is translated into the appropriate pattern of transcriptional output.

METHODS

Plant Materials and Growth Conditions

The Colombia-0 ecotype of *Arabidopsis thaliana* was used for all experiments. The transgenic line PIL5OX (P1M) (Oh et al., 2006), 35S:6xHis-PIF3-5xMYC (P3M) (Al-Sady et al., 2006), *pif1-1* (Huq et al., 2004), *pif3* (Monte et al., 2004), *pif5-3* (Khanna et al., 2007), *pif1pif4pif5* (*pif145*) (Leivar et al., 2012), *pif4-2*, *pif1pif3pif4* (*pif134*), *pif1pif3pif5* (*pif135*), *pif3pif4pif5* (*pif345*), and *pif1pif3pif4pif5* (*pifq*) (Leivar et al., 2008) were described earlier.

Generation of 35S:PIF4-MYC (P4M) Transgenic Plants

The full-length coding sequence (cds) of PIF4 was amplified by PCR using the PIF4-CF1/CR1 primer set—PIF4-CF1: tcagtcgacATGGAACACCAAGGTTGGAGTTTTG, PIF4-CR1: tcagcggccgcgaGTGGTCCAAACGAGAACCGTCG—and then the *Sal*I/*Not*I fragment was cloned into the pENTR4 vector (Invitrogen) to produce the pENTR4–PIF4 entry clone. The PIF4 cds was subcloned into the gateway-compatible pGWB17 binary vector (Nakagawa et al., 2007) using Gateway LR Clonase II Enzyme Mix (Invitrogen) to produce the pGWB17–PIF4 (35S:PIF4–Myc) construct. This construct was transformed into *Arabidopsis pif4-2*-mutant (Leivar et al., 2008) plants as described (Zhang et al., 2006), and the individual transgenic lines were selected on MS medium containing 25 mg L^{-1} of Hygromycin B (Invitrogen).

ChIP-Seq Library Construction and Data Processing

ChIP assays were performed using dark-grown WT, PIF1-myc-, and PIF4-myc-expressing seedlings (0.2 g seed weight each) as described earlier (Gendrel et al., 2005; Zhang et al., 2013). We used 2-day-old seedlings for the PIF4- and corresponding WT–ChIP analyses, and 3-day-old seedlings for the PIF1- and corresponding WT–ChIP analyses. Enrichment of specific DNA fragments was validated by RT–qPCR, using conditions and primers as specified earlier (Zhang et al., 2013). Two biological replicates were prepared for each PIF-ChIP and each WT control ChIP sample. Three independent libraries were generated for each replicate using pooled DNA from four ChIP preparations. For this purpose, the NEXTflex ChIP-seq kit and 6 NEXTflex ChIP-Seq Barcodes (Bioo Scientific) were used, according to the manufacturer's instructions. Adapter-ligated DNA fragments of 200–300 bp were gel-purified, validated by Bioanalyzer 2000 (Agilent), and quantified by the KAPA Library Quantification Kit (KAPABiosystems). Six independently bar-coded libraries were pooled in a single lane and sequenced by 50-cycle single-end sequencing on the Illumina HiSeq platform.

All reads were mapped to chromosomes 1–5 of the TAIR10 genome using Bowtie (Langmead et al., 2009) with the following flags –v 2 —best —strata –m 1 –5 3. Identification of binding sites was performed independently for each biological replicate using MACS (Zhang et al., 2008) with default settings and the following options: –f BOWTIE –g 1.5e8 —off–auto —nomodel —shiftsize=60 –w –S. Binding summits were considered reproducible between biological replicates when located within 100 bp of each other. For each reproducible binding region, a new mean summit position was calculated at the average position of the individual summits and subsequently extended equally on both sides to define a 200-bp binding site.

De novo motif analysis within binding sites was performed using DREME (Bailey et al., 2011). The web-based analysis tool Galaxy (Blankenberg et al., 2001; Giardine et al., 2005; Goecks et al., 2010) was used for all operations on genomic intervals and the annotation of genes

associated with binding sites. PIF5 ChIP-seq analysis was based on raw sequences only that were published earlier (Hornitschek et al., 2012) and done as described for PIF1 and PIF4, except that no biological replicates were available for this experiment.

RNA-Seq Library Construction and Data Processing

Total RNA from 2-day-old dark-grown seedlings was extracted as described in Zhang et al. (2013). Sequencing libraries were also prepared as described by these authors except that RNA-Seq Barcode Primers (Epicentre Biotechnologies) were introduced during PCR amplification of the first-strand cDNA. Libraries were quantitated using the KAPA Library Quantification Kit (KAPABiosystems).

Libraries from triplicate biological samples were assayed by 50-cycle single-end sequencing on the Illumina HiSeq platform. Reads were aligned to the TAIR9 representative transcriptome using Bowtie (Langmead et al., 2009) with zero mismatches allowed. Only reads mapping uniquely to the 3′-end 500-bp region of the coding strand were counted for gene expression. Differentially expressed genes were identified using the edgeR package (Robinson et al., 2010), and SSTF genes were defined as those that differ by at least two-fold with an adjusted *P*-value ≤ 0.05 as described (Leivar et al., 2009).

Electrophoretic Mobility Shift Assays (EMSAs)

EMSAs were performed as described earlier (Martínez-García et al., 2000). PIF1 was produced with a TnT rabbit reticulocyte lysate system (Promega) using the PIF1 cDNA cloned in the pT7CFE1 vector (Thermo Scientific) as a template. GFP was produced the same way using pCFE–GFP (Thermo Scientific) as template. To generate double-stranded probes, the complementary oligonucleotides (IDT) listed in Supplemental Table 7 were diluted in annealing buffer (10 mM Tris–HCl (pH 7.5), 50 mM NaCl, 1 mM EDTA) to a final concentration of 40 μM each, heated to 95°C for 5 min, and cooled down slowly (0.1°C s^{-1}) to 12°C. Probes were further labeled with [32P]-γ-ATP, using T4 polynucleotide kinase (NEB), and purified by gel filtration through Sephadex G-25. Labeled probes were used at a final concentration of 2500 cpm μl^{-1} and all competitor probes at 0.25 μM.

Accession Numbers

ChIP-seq and RNA-seq data reported in this study have been deposited in the Gene Expression Omnibus database under the accession number GSE43286. The previous data from Zhang et al. (2013) are under the number GSE39217.

SUPPLEMENTARY DATA

Supplementary Data are available at *Molecular Plant Online.*

FUNDING

This work was supported by a Feodor Lynen Research Fellowship from the Alexander von Humboldt Foundation to A.P., a China Scholarship Council fellowship to H.S., and by National Institutes of Health Grant GM-R01-47475, Department of Energy Grant DE-FG03-87ER13742, and USDA Agricultural Research Service Current Research Information System Grant 5335–21000–032–00D to P.H.Q.

ACKNOWLEDGMENTS

We thank our lab colleagues for valuable discussions, Elena Monte for comments on the manuscript, the Functional Genomics Laboratory at UC-Berkeley and Madhavan Ganesh at the Computational Genomics Resource Laboratory at UC-Berkeley, and E. Oh and G. Choi for the *Arabidopsis* line PIL5OX (P1M) used for PIF1 ChIP-seq analysis. No conflict of interest declared.

REFERENCES

Al-Sady, B., Kikis, E.A., Monte, E., and Quail, P.H. (2008). Mechanistic duality of transcription factor function in phytochrome signaling. Proc. Natl Acad. Sci. U S A. **105**, 2232–2237.

Al-Sady, B., Ni, W., Kircher, S., Schäfer, E., and Quail, P.H. (2006). Photoactivated phytochrome induces rapid PIF3 phosphorylation prior to proteasome-mediated degradation. Mol. Cell. **23**, 439–446.

Bae, G., and Choi, G. (2008). Decoding of light signals by plant phytochromes and their interacting proteins. Annu. Rev. Plant Biol. **59**, 281–311.

Bai, M.-Y., Shang, J.-X., Oh, E., Fan, M., Bai, Y., Zentella, R., Sun, T.-p., and Wang, Z.-Y. (2012). Brassinosteroid, gibberellin and phytochrome impinge on a common transcription module in *Arabidopsis*. Nat. Cell Biol. **14**, 810–814.

Bailey, T.L., Williams, N., Misleh, C., and Li, W.W. (2006). MEME: discovering and analyzing DNA and protein sequence motifs. Nucleic Acids Res. **34**, W369–W373.

Bailey, T.L., Williams, N., Misleh, C., and Li, W.W. (2011). DREME: motif discovery in transcription factor ChIP-seq data. Bioinformatics. **27**, 1653–1659.

Bauer, D., Viczian, A., Kircher, S., Nobis, T., Nitschke, R., Kunkel, T., Panigrahi, K.C.S., Adam, E., Fejes, E., Schäfer, E., et al. (2004). Constitutive Photomorphogenesis 1 and multiple photoreceptors control degradation of Phytochrome Interacting Factor 3, a

transcription factor required for light signaling in *Arabidopsis*. Plant Cell. **16**, 1433–1445.

Biggin, M.D. (2011). Animal transcription networks as highly connected, quantitative continua. Dev. Cell. **21**, 611–626.

Blankenberg, D., Kuster, G.V., Coraor, N., Ananda, G., Lazarus, R., Mangan, M., Nekrutenko, A., and Taylor, J. (2010). Galaxy: a web-based genome analysis tool for experimentalists. In Current Protocols in Molecular Biology, Ausubel, F.M., Brent, R., Kingston, R.E., Moore, D.D., Seidman, J.G., Smith, J.A., and Struhl, K., eds. (Chichester, UK: John Wiley & Sons, Inc.).

Boros, J., O'Donnell, A., Donaldson, I.J., Kasza, A., Zeef, L., and Sharrocks, A.D. (2009). Overlapping promoter targeting by Elk-1 and other divergent ETS-domain transcription factor family members. Nucleic Acids Res. **37**, 7368–7380.

Boyd, K.E., Wells, J., Gutman, J., Bartley, S.M., and Farnham, P.J. (1998). c-Myc target gene specificity is determined by a post-DNAbinding mechanism. Proc. Natl Acad. Sci. U S A. **95**, 13887–13892.

Castillon, A., Shen, H., and Huq, E. (2007). Phytochrome interacting factors: central players in phytochrome-mediated light signaling networks. Trends Plant Sci. **12**, 514–521.

Chang, K.N., Zhong, S., Weirauch, M.T., Hon, G., Pelizzola, M., Li, H., Huang, S.S., Schmitz, R.J., Urich, M.A., Kuo, D., et al. (2013). Temporal transcriptional response to ethylene gas drives growth hormone cross-regulation in *Arabidopsis*. eLife. **2**, e00675.

Cheng, C., Alexander, R., Min, R., Leng, J., Yip, K.Y., Rozowsky, J., Yan, K.-K., Dong, X., Djebali, S., Ruan, Y., et al. (2012). Understanding transcriptional regulation by integrative analysis of transcription factor binding data. Genome Res. **22**, 1658–1667.

de Lucas, M., Daviere, J.M., Rodriguez-Falcon, M., Pontin, M., Iglesias-Pedraz, J.M., Lorrain, S., Fankhauser, C., Blazquez, M.A., Titarenko, E., and Prat, S. (2008). A molecular framework for light and gibberellin control of cell elongation. Nature. **451**, 480–484.

Duek, P.D., and Fankhauser, C. (2005). bHLH class transcription factors take centre stage in phytochrome signalling. Trends Plant Sci. **10**, 51–54.

Farnham, P.J. (2009). Insights from genomic profiling of transcription factors. Nat. Rev. Genet. **10**, 605–616.

Feng, S., Martinez, C., Gusmaroli, G., Wang, Y., Zhou, J., Wang, F., Chen, L., Yu, L., Iglesias-Pedraz, J.M., Kircher, S., et al. (2008). Coordinated regulation of *Arabidopsis thaliana* development by light and gibberellins. Nature. **451**, 475–479.

Ferrier, T., Matus, J.T.s., Jin, J., and Riechmann, J.L. (2011). *Arabidopsis* paves the way: genomic and network analyses in crops. Curr. Opin. Biotechnol. **22**, 260–270.

Fisher, W.W., Li, J.J., Hammonds, A.S., Brown, J.B., Pfeiffer, B.D., Weiszmann, R., MacArthur, S., Thomas, S., Stamatoyannopoulos, J.A., Eisen, M.B., et al. (2012). DNA regions bound at low occupancy by transcription factors do not drive patterned reporter gene expression in *Drosophila*. Proc. Natl Acad. Sci. U S A. **109**, 21330–21335.

Franklin, K.A., and Quail, P.H. (2010). Phytochrome functions in *Arabidopsis* development. J. Exp. Bot. **61**, 11–24.

Franklin, K.A., Lee, S.H., Patel, D., Kumar, S.V., Spartz, A.K., Gu, C., Ye, S., Yu, P., Breen, G., Cohen, J.D., et al. (2011). PHYTOCHROME-INTERACTING FACTOR 4 (PIF4) regulates auxin biosynthesis at high temperature. Proc. Natl Acad. Sci. U S A. **108**, 20231–20235.

Gendrel, A.-V., Lippman, Z., Martienssen, R., and Colot, V. (2005). Profiling histone modification patterns in plants using genomic tiling microarrays. Nature Methods. **2**, 213–218.

Giardine, B., Riemer, C., Hardison, R.C., Burhans, R., Elnitski, L., Shah, P., Zhang, Y., Blankenberg, D., Albert, I., Taylor, J., et al. (2005). Galaxy: a platform for interactive large-scale genome analysis. Genome Res. **15**, 1451–1455.

Goecks, J., Nekrutenko, A., Taylor, J., and The Galaxy, T. (2010). Galaxy: a comprehensive approach for supporting accessible, reproducible, and transparent computational research in the life sciences. Genome Biol. **11**, R86.

Gordan, R., Shen, N., Dror, I., Zhou, T., Horton, J., Rohs, R., and Bulyk, M.L. (2013). Genomic regions flanking E-box binding sites influence DNA binding specificity of bHLH transcription factors through DNA shape. Cell Reports. **3**, 1093–1104.

Hahn, S., and Young, E.T. (2011). Transcriptional regulation in *Saccharomyces cerevisiae*: transcription factor regulation and function, mechanisms of initiation, and roles of activators and coactivators. Genetics. **189**, 705–736.

Hao, Y., Oh, E., Choi, G., Liang, Z., and Wang, Z.-Y. (2012). Interactions between HLH and bHLH factors modulate light-regulated plant development. Mol. Plant. **5**, 688–697.

Hollenhorst, P.C., Shah, A.A., Hopkins, C., and Graves, B.J. (2007). Genome-wide analyses reveal properties of redundant and specific promoter occupancy within the ETS gene family. Genes Dev. **21**, 1882–1894.

Hornitschek, P., Kohnen, M.V., Lorrain, S., Rougemont, J., Ljung, K., Lopez-Vidriero, I., Franco-Zorrilla, J.M., Solano, R., Trevisan, M., Pradervand, S., et al. (2012). Phytochrome interacting factors 4 and 5 control seedling growth in changing light conditions by directly controlling auxin signaling. Plant J. **71**, 699–711.

Hornitschek, P., Lorrain, S., Zoete, V., Michielin, O., and Fankhauser, C. (2009). Inhibition of the shade avoidance response by formation of non-DNA binding bHLH heterodimers. EMBO J. **28**, 3893–3902.

Huq, E., Al-Sady, B., Hudson, M., Kim, C., Apel, K., and Quail, P.H. (2004). PHYTOCHROME-INTERACTING FACTOR 1, a basic helix–loop–helix transcription factor, is a critical regulator of the chlorophyll biosynthetic pathway. Science. **305**, 1937–1941.

Jiao, Y., Lau, O.S., and Deng, X.W. (2007). Light-regulated transcriptional networks in higher plants. Nat. Rev. Genet. **8**, 217–230.

Khanna, R., Shen, Y., Marion, C.M., Tsuchisaka, A., Theologis, A., Schafer, E., and Quail, P.H. (2007). The basic helix–loop–helix transcription factor PIF5 acts on ethylene biosynthesis and phytochrome signaling by distinct mechanisms. Plant Cell. **19**, 3915–3929.

Kininis, M., Chen, B.S., Diehl, A.G., Clark, A.G., Isaacs, G.D., Zhang, T., Siepel, A.C., and Kraus, W.L. (2007). Genomic analyses of transcription factor binding, histone acetylation, and gene expression reveal mechanistically distinct classes of estrogen-regulated promoters. Mol. Cell. Biol. **27**, 5090–5104.

Koini, M.A., Alvey, L., Allen, T., Tilley, C.A., Harberd, N.P., Whitelam, G.C., and Franklin, K.A. (2009). High temperature-mediated adaptations in plant architecture require the bHLH transcription factor PIF4. Curr. Biol. **19**, 408–413.

Langmead, B., Trapnell, C., Pop, M., and Salzberg, S. (2009). Ultrafast and memory-efficient alignment of short DNA sequences to the human genome. Genome Biol. **10**, R25.

Leivar, P., and Quail, P.H. (2011). PIFs: pivotal components in a cellular signaling hub. Trends in Plant Science **16**, 19–28.

Leivar, P., Monte, E., Oka, Y., Liu, T., Carle, C., Castillon, A., Huq, E., and Quail, P.H. (2008). Multiple phytochrome-interacting bHLH transcription factors repress premature seedling photomorphogenesis in darkness. Curr. Biol. **18**, 1815–1823.

Leivar, P., Tepperman, J.M., Cohn, M.M., Monte, E., Al-Sady, B., Erickson, E., and Quail, P.H. (2012). Dynamic antagonism between phytochromes and PIF family basic helix-loop-helix factors induces selective reciprocal responses to light and shade in a rapidly responsive transcriptional network in *Arabidopsis*. The Plant Cell Online. **24**, 1398–1419.

Leivar, P., Tepperman, J.M., Monte, E., Calderon, R.H., Liu, T.L., and Quail, P.H. (2009). Definition of early transcriptional circuitry involved in light-induced reversal of PIF-imposed repression of photomorphogenesis in young *Arabidopsis* seedlings. Plant Cell. **21**, 3535–3553.

Li, L., Ljung, K., Breton, G., Schmitz, R.J., Pruneda-Paz, J., Cowing-Zitron, C., Cole, B.J., Ivans, L.J., Pedmale, U.V., Jung, H.-S., et al. (2012). Linking photoreceptor excitation to changes in plant architecture. Genes Dev. **26**, 785–790.

Li, X.-Y., Thomas, S., Sabo, P., Eisen, M., Stamatoyannopoulos, J., and Biggin, M. (2011). The role of chromatin accessibility in directing the widespread, overlapping patterns of *Drosophila* transcription factor binding. Genome Biol. **12**, R34.

Lickwar, C.R., Mueller, F., Hanlon, S.E., McNally, J.G., and Lieb, J.D. (2012). Genome-wide protein–DNA binding dynamics suggest a molecular clutch for transcription factor function. Nature. **484**, 251–255.

Liu, X., Chen, C.-Y., Wang, K.-C., Luo, M., Tai, R., Yuan, L., Zhao, M., Yang, S., Tian, G., Cui, Y., et al. (2013). PHYTOCHROME INTERACTING FACTOR3 associates with the histone deacetylase HDA15 in repression of chlorophyll biosynthesis and photosynthesis in etiolated *Arabidopsis* seedlings. The Plant Cell Online. **25**, 1258–1273.

Lorrain, S., Allen, T., Duek, P.D., Whitelam, G.C., and Fankhauser, C. (2008). Phytochrome-mediated inhibition of shade avoidance involves degradation of growth-promoting bHLH transcription factors. Plant J. **53**, 312–323.

Lorrain, S., Trevisan, M., Pradervand, S., and Fankhauser, C. (2009). Phytochrome interacting factors 4 and 5 redundantly limit seedling de-etiolation in continuous far-red light. Plant J. **60**, 449–461.

Lucyshyn, D., and Wigge, P.A. (2009). Plant development: PIF4 integrates diverse environmental signals. Curr. Biol. **19**, R265–R266.

MacArthur, S., Li, X.-Y., Li, J., Brown, J., Chu, H.C., Zeng, L., Grondona, B., Hechmer, A., Simirenko, L., Keranen, S., et al. (2009). Developmental roles of 21 *Drosophila* transcription factors are determined by quantitative differences in binding to an overlapping set of thousands of genomic regions. Genome Biol. **10**, R80.

Martínez-García, J.F., Huq, E., and Quail, P.H. (2000). Direct targeting of light signals to a promoter element-bound transcription factor. Science. **288**, 859–863.

Monte, E., Tepperman, J.M., Al-Sady, B., Kaczorowski, K.A., Alonso, J.M., Ecker, J.R., Li, X., Zhang, Y., and Quail, P.H. (2004). The phytochrome-interacting transcription factor, PIF3, acts early, selectively, and positively in light-induced chloroplast development. Proc. Natl Acad. Sci. U S A. **101**, 16091–16098.

Moon, J., Zhu, L., Shen, H., and Huq, E. (2008). PIF1 directly and indirectly regulates chlorophyll biosynthesis to optimize the greening process in *Arabidopsis*. Proc. Natl Acad. Sci. U S A. **105**, 9433–9438.

Nagatani, A. (2004). Light-regulated nuclear localization of phytochromes. Curr. Opin. Plant Biol. **7**, 708–711.

Nakagawa, T., Kurose, T., Hino, T., Tanaka, K., Kawamukai, M., Niwa, Y., Toyooka, K., Matsuoka, K., Jinbo, T., and Kimura, T. (2007). Development of series of gateway binary vectors, pGWBs, for realizing efficient construction of fusion genes for plant transformation. Journal of Bioscience and Bioengineering. **104**, 34–41.

Ni, W., Xu, S.L., Chalkley, R.J., Pham, T.N., Guan, S., Maltby, D.A., Burlingame, A.L., Wang, Z.Y., and Quail, P.H. (2013). Multisite light-induced phosphorylation of the transcription factor PIF3 is necessary for both its rapid degradation and concomitant negative feedback modulation of photoreceptor phyB levels in *Arabidopsis*. Plant Cell. **25**, 2679–2698.

Niwa, Y., Yamashino, T., and Mizuno, T. (2009). The circadian clock regulates the photoperiodic response of hypocotyl elongation through a coincidence mechanism in *Arabidopsis thaliana*. Plant Cell Physiol. **50**, 838–854.

Nozue, K., Covington, M.F., Duek, P.D., Lorrain, S., Fankhauser, C., Harmer, S.L., and Maloof, J.N. (2007). Rhythmic growth explained by coincidence between internal and external cues. Nature. **448**, 358–361.

Oh, E., Kang, H., Yamaguchi, S., Park, J., Lee, D., Kamiya, Y., and Choi, G. (2009). Genome-wide analysis of genes targeted by PHYTOCHROME INTERACTING FACTOR 3-LIKE5 during seed germination in *Arabidopsis*. The Plant Cell Online. **21**, 403–419.

Oh, E., Yamaguchi, S., Kamiya, Y., Bae, G., Chung, W.I., and Choi, G. (2006). Light activates the degradation of PIL5 protein to promote seed germination through gibberellin in *Arabidopsis*. Plant J. **47**, 124–139.

Oh, E., Zhu, J.Y., and Wang, Z.Y. (2012). Interaction between BZR1 and PIF4 integrates brassinosteroid and environmental responses. Nat. Cell Biol. **14**, 802–809.

Ouyang, Z., Zhou, Q., and Wong, W.H. (2009). ChIP-seq of transcription factors predicts absolute and differential gene expression in embryonic stem cells. Proc. Natl Acad. Sci. U S A. **106**, 21521–21526.

Park, E., Kim, J., Lee, Y., Shin, J., Oh, E., Chung, W.-I., Liu, J.R., and Choi, G. (2004). Degradation of phytochrome interacting factor 3 in phytochrome-mediated light signaling. Plant Cell Physiol. **45**, 968–975.

Pfeiffer, A., Nagel, M.-K., Popp, C., Wüst F, F., Bindics, J.N., Viczián, A.s., Hiltbrunner, A., Nagy, F., Kunkel, T., and Schäfer, E. (2012). Interaction with plant transcription factors can mediate nuclear import of phytochrome B. Proc. Natl Acad. Sci. U S A. **109**, 5892–5897.

Quail, P.H. (2002). Phytochrome photosensory signalling networks. Nat. Rev. Mol. Cell Biol. **3**, 85–93.

Quail, P.H. (2007). Phytochrome interacting factors. In Light and Plant Development, **Whitelam, G.C. and Halliday, K.J.**, eds (Oxford, UK: Blackwell Publishing), pp. 81–105.

Robinson, M.D., McCarthy, D.J., and Smyth, G.K. (2010). edgeR: a bioconductor package for differential expression analysis of digital gene expression data. Bioinformatics. **26**, 139–140.

Rockwell, N.C., Su, Y.S., and Lagarias, J.C. (2006). Phytochrome structure and signaling mechanisms. Annu. Rev. Plant Biol. **57**, 837–858.

Roig-Villanova, I., Bou, J., Sorin, C.I., Devlin, P.F., and Martínez-García, J.F. (2006). Identification of primary target genes of phytochrome signaling: early transcriptional control during shade avoidance responses in *Arabidopsis*. Plant Physiol. **141**, 85–96.

Schäfer, E., and Nagy, F. (2006). Photomorphogenesis in Plants and Bacteria (Dordrecht, The Netherlands: Springer).

Sentandreu, M., Martin, G., González-Schain, N., Leivar, P., Soy, J., Tepperman, J.M., Quail, P.H., and Monte, E. (2011). Functional profiling identifies genes involved in organ-specific branches of the PIF3 regulatory network in *Arabidopsis*. The Plant Cell Online. **23**, 3974–3991.

Shen, H., Moon, J., and Huq, E. (2005). PIF1 is regulated by light-mediated degradation through the ubiquitin-26S proteasome pathway to optimize photomorphogenesis of seedlings in *Arabidopsis*. Plant J. **44**, 1023–1035.

Shen, H., Zhu, L., Castillon, A., Majee, M., Downie, B., and Huq, E. (2008). Light-induced phosphorylation and degradation of the negative regulator PHYTOCHROME-INTERACTING FACTOR1 from *Arabidopsis* depend upon its direct physical interactions with photoactivated phytochromes. Plant Cell. **20**, 1586–1602.

Shen, Y., Khanna, R., Carle, C.M., and Quail, P.H. (2007). Phytochrome induces rapid PIF5 phosphorylation and degradation in response to red-light activation. Plant Physiol. **145**, 1043–1051.

Shin, J., Kima, K., Kang, H., Zulfugarovc, I. S., Baea, G., Leec, C.-H., Leeb, D., and Choi, C. (2009). Phytochromes promote seedling light responses by inhibiting four negatively-acting phytochrome-interacting factors. PNAS. **106**, 7660–7665.

Soy, J., Leivar, P., González-Schain, N., Sentandreu, M., Prat, S., Quail, P.H., and Monte, E. (2012). Phytochrome-imposed oscillations in PIF3 protein abundance regulate hypocotyl growth under diurnal light/dark conditions in *Arabidopsis*. Plant J. **71**, 390–401.

Stewart, J.L., Maloof, J.N., and Nemhauser, J.L. (2011). *PIF* genes mediate the effect of sucrose on seedling growth dynamics. PLoS ONE. **6**, e19894.

Sun, Y., Fan, X.-Y., Cao, D.-M., Tang, W., He, K., Zhu, J.-Y., He, J.-X., Bai, M.-Y., Zhu, S., Oh, E., et al. (2010). Integration of brassinosteroid signal transduction with the transcription network for plant growth regulation in *Arabidopsis*. Dev. Cell. **19**, 765–777.

Tao, Z., Shen, L., Liu, C., Liu, L., Yan, Y., and Yu, H. (2012). Genome-wide identification of SOC1 and SVP targets during the floral transition in *Arabidopsis*. Plant J. **70**, 549–561.

Toledo-Ortiz, G., Huq, E., and Quail, P.H. (2003). The *Arabidopsis* basic helix–loop–helix transcription factor family. Plant Cell. **15**, 1749–1770.

Wang, H., and Deng, X.W. (2003). Dissecting the phytochrome A-dependent signaling network in higher plants. Trends Plant Sci. **8**, 172–178.

Weinmann, A.S., Bartley, S.M., Zhang, T., Zhang, M.Q., and Farnham, P.J. (2001). Use of chromatin immunoprecipitation to clone novel E2F target promoters. Mol. Cell Biol. **21**, 6820–6832.

Xie, W., Schultz, M.D., Lister, R., Hou, Z., Rajagopal, N., Ray, P., Whitaker, J.W., Tian, S., Hawkins, R.D., Leung, D., et al. (2013). Epigenomic analysis of multilineage differentiation of human embryonic stem cells. Cell. **153**, 1134–1148.

Xu, X., Bieda, M., Jin, V.X., Rabinovich, A., Oberley, M.J., Green, R., and Farnham, P.J. (2007). A comprehensive ChIP-chip analysis of E2F1, E2F4, and E2F6 in normal and tumor cells reveals interchangeable roles of E2F family members. Genome Res. **17**, 1550–1561.

Yu, X., Li, L., Zola, J., Aluru, M., Ye, H., Foudree, A., Guo, H., Anderson, S., Aluru, S., Liu, P., et al. (2011). A brassinosteroid transcriptional network revealed by genome-wide identification of BESI target genes in *Arabidopsis thaliana*. Plant J. **65**, 634–646.

Zhang, H., He, H., Wang, X., Wang, X., Yang, X., Li, L., and Deng, X.W. (2011). Genome-wide mapping of the HY5-mediated genenetworks in *Arabidopsis* that involve both transcriptional and post-transcriptional regulation. Plant J. **65**, 346–358.

Zhang, X., Henriques, R., Lin, S.-S., Niu, Q.-W., and Chua, N.-H. (2006). Agrobacterium-mediated transformation of *Arabidopsis thaliana* using the floral dip method. Nature Protocols. **1**, 641–646.

Zhang, Y., Liu, T., Meyer, C.A., Eeckhoute, J., Johnson, D.S., Bernstein, B.E., Nusbaum, C., Myers, R.M., Brown, M., Li, W.,

et al. (2008). Model-based analysis of ChIP-seq (MACS). Genome Biol. **9**, R137.

Zhang, Y., Mayba, O., Pfeiffer, A., Shi, H., Tepperman, J.M., Speed, T.P., and Quail, P.H. (2013). A quartet of PIF bHLH factors provides a transcriptionally centered signaling hub that regulates seedling morphogenesis through differential expression-patterning of shared target genes in *Arabidopsis*. PLoS Genet. **9**, e1003244.

Zhong, S., Shi, H., Xue, C., Wang, L., Xi, Y., Li, J., Quail, P.H., Deng, X.W., and Guo, H. (2012). A molecular framework of light-controlled phytohormone action in *Arabidopsis*. Curr. Biol. **22**, 1530–1535.

Zhou, X., and O'Shea, E.K. (2011). Integrated approaches reveal determinants of genome-wide binding and function of the transcription factor Pho4. Mol. Cell. **42**, 826–836.